# Local subcell monolithic DG/FV scheme

**François Vilar**

Institut Montpelliérain Alexander Grothendieck, Université de Montpellier, France

**Séminaire CEA-GAMNI**


## Scalar Conservation Law (SCL)

- $\partial_t u(\mathbf{x},t) + \nabla_x \cdot \mathbf{F}(u(\mathbf{x},t)) = 0, \qquad (\mathbf{x},t) \in \mathbb{R}^d \times [0,T]$
- $u(\mathbf{x},0) = u_0(\mathbf{x}), \qquad \mathbf{x} \in \mathbb{R}^d$

## Fundamental difficulty

- **Even considering smooth flux function $F(\cdot)$ and initial datum $u_0(\cdot)$ ($\mathcal{C}^\infty$ for instance), solution may become discontinuous in finite time**
- Standard example: Burgers equation

$$\begin{cases} \partial_t u + \partial_x\left(\frac{1}{2}u^2\right) = 0, & (x,t) \in [0,1] \times \mathbb{R}^+, \\ u(x,0) = \sin(2\pi x), & x \in [0,1]. \end{cases}$$

## Strong solution

- Local in time existence and uniqueness of a solution $u \in \mathcal{C}^1\left(\mathbb{R}^d \times [0,\, t_c[\,\right)$

# Formation of a discontinuity in finite time

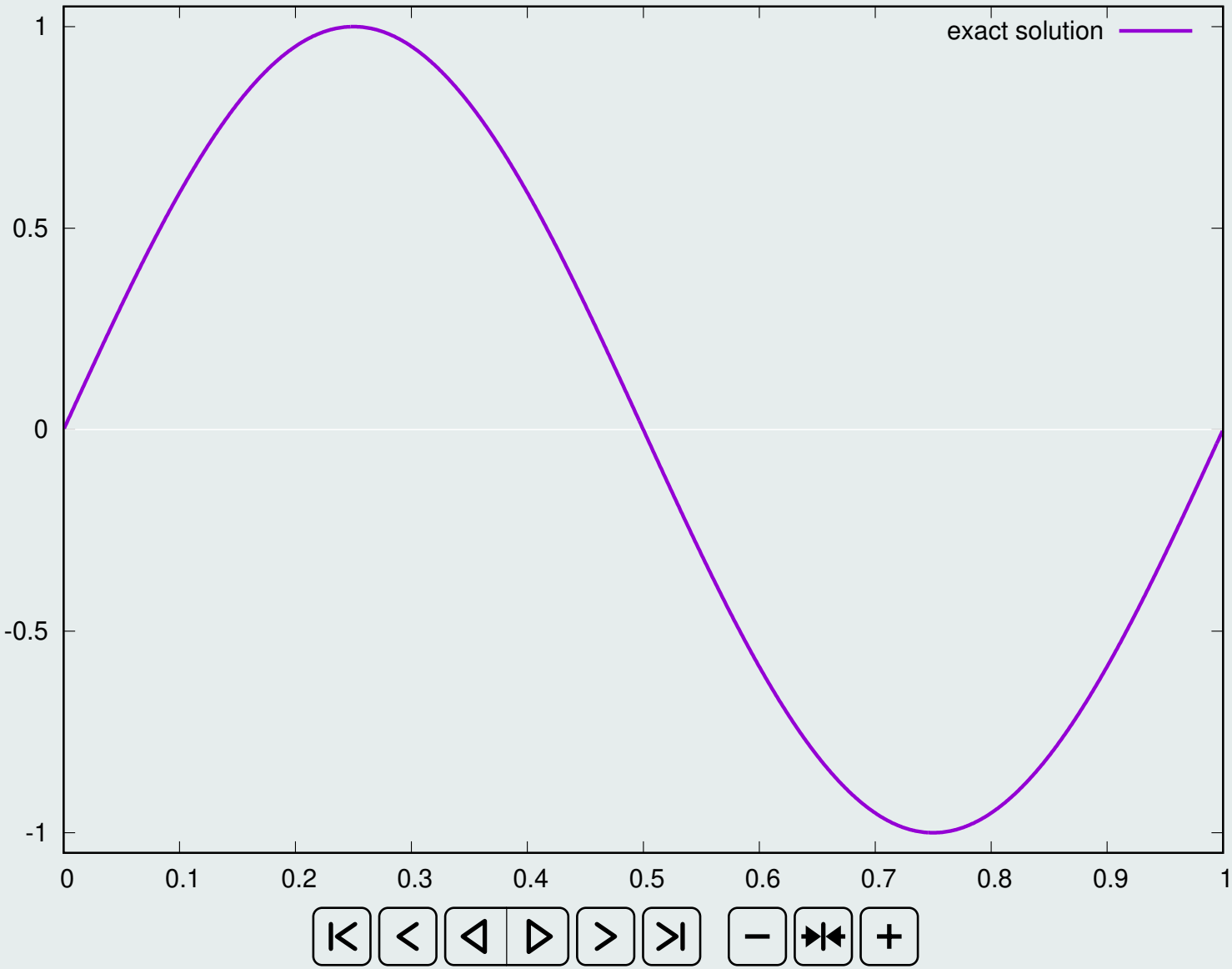

## Weak solution

$\forall\, \psi \in \mathcal{C}_0^1(\mathbb{R}^d \times \mathbb{R}^+)$

- $$\int \int_{\mathbb{R}^d \times \mathbb{R}^+} \Big( u\, \partial_t \psi + \boldsymbol{F}(u) \,.\, \nabla_x \psi \Big)\, \mathrm{d}\boldsymbol{x}\, \mathrm{d}t - \int_{\mathbb{R}^d} u_0(\boldsymbol{x})\, \psi(\boldsymbol{x}, 0)\, \mathrm{d}\boldsymbol{x} = 0$$
- Non-uniqueness of a weak solution $u \in L^\infty_{loc}(\mathbb{R}^d \times \mathbb{R}^+)$

## Entropy definition

- Let $u \in \mathcal{C}^1\big(\mathbb{R}^d \times [0,\, t_c[\,\big)$ be a strong solution
- $\eta$ a strictly convex function is an entropy if $\exists\, \phi$ s.t.

$$\partial_t\, \eta(u) + \nabla_x \,.\, \phi(u) = 0$$

## Unique entropic weak solution

$\forall\, \psi \in \mathcal{C}_0^1(\mathbb{R}^d \times \mathbb{R}^+)$

- Let $u \in L^\infty_{loc}\big(\mathbb{R}^d \times \mathbb{R}^+\big)$ be a weak solution
- $u$ is the unique entropic weak solution if it satisfies, for any pair $(\eta, \phi)$

$$\int \int_{\mathbb{R}^d \times \mathbb{R}^+} \Big( \eta(u)\, \partial_t \psi + \phi(u) \,.\, \nabla_x \psi \Big)\, \mathrm{d}\boldsymbol{x}\, \mathrm{d}t - \int_{\mathbb{R}^d} \eta\big(u_0(\boldsymbol{x})\big)\, \psi(\boldsymbol{x}, 0)\, \mathrm{d}\boldsymbol{x} \geq 0$$

# Formation of a discontinuity in finite time

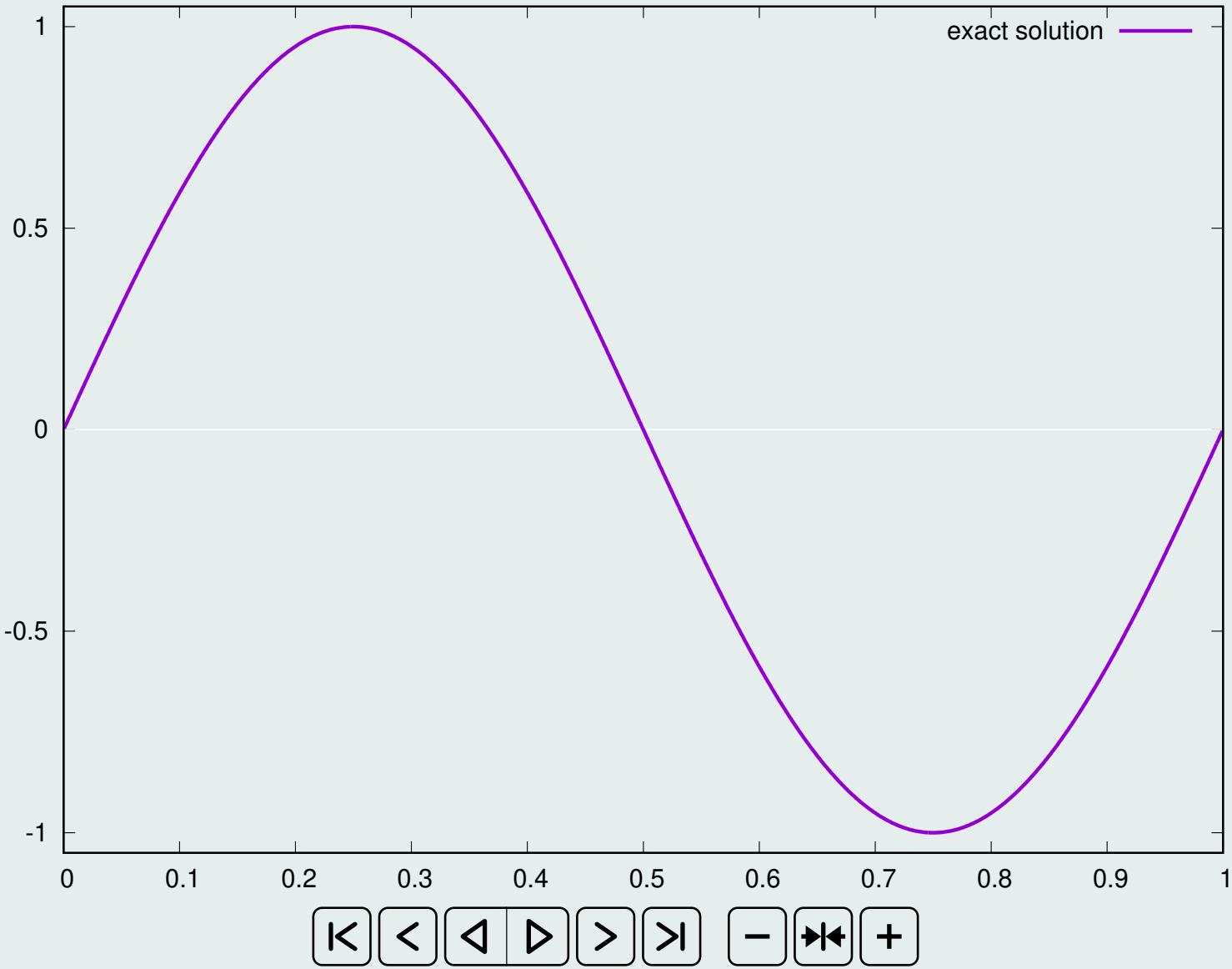

## Challenges of numerical discretization

- **The weak solution we wish to approach may present areas of great regularity as well as discontinuities of great intensity**

$\longrightarrow$ **Smooth areas**: high accuracy

$\longrightarrow$ **Discontinuities**: strong robustness and stability

$\longrightarrow$ **Everywhere**: additional mathematical or physical constraints

$\hookrightarrow$ Maximum principle or positivity

$\hookrightarrow$ Entropy inequalities

$\hookrightarrow$ ...

## Numerical schemes and discontinuous approximated solution

- **Finite Volume** **FV**
- (Weighted) Essentially Non-Oscillatory (W)-ENO
- **Discontinuous Galerkin** **DG**

## Discontinuous Galerkin scheme

- Introduced by Reed and Hill in 1973 in the frame of the neutron transport
- Major development and improvements by B. Cockburn and C.-W. Shu

## Procedure

- Local variational formulation
- Piecewise polynomial approximation of the solution in the cells
- Choice of the numerical fluxes
- Time integration

## Advantages

- Natural extension of Finite Volume method
- Excellent analytical properties ($L_2$ stability, $hp-$adaptivity, ...)
- Extremely high accuracy (superconvergent for scalar conservation laws)
- Compact stencil (involve only face neighboring cells)

## Scalar conservation law

- $\partial_t u(\mathbf{x},t) + \nabla_x \cdot \mathbf{F}(u(\mathbf{x},t)) = 0, \qquad (\mathbf{x},t) \in \omega \times [0,T]$
- $u(\mathbf{x},0) = u_0(\mathbf{x}), \qquad \mathbf{x} \in \omega$

## $(k+1)^{\text{th}}$ order semi-discretization

- $\{\omega_c\}_c$ a partition of $\omega$, such that $\omega = \bigcup_c \omega_c$
- $u_h(\mathbf{x},t)$ the numerical solution, such that $u_{h|\omega_c} = u_h^c \in \mathbb{P}^k(\omega_c)$

$$u_h^c(\mathbf{x},t) = \sum_{m=1}^{N_k} u_m^c(t)\,\sigma_m^c(\mathbf{x})$$

- $\{\sigma_m^c\}_{m=1,\dots,N_k}$ a basis of $\mathbb{P}^k(\omega_c)$, with $N_k = \frac{(k+1)(k+2)}{2}$ in 2D.

## Local variational formulation on $\omega_c$

- $\displaystyle\int_{\omega_c} \frac{\partial u_h^c}{\partial t}\,\psi \,\mathrm{d}V = \oint_{\omega_c} \mathbf{F}(u_h^c) \cdot \nabla_x \psi \,\mathrm{d}V - \oint_{\partial\omega_c} \psi\, \mathcal{F}_n \,\mathrm{d}S, \qquad \forall\, \psi \in \mathbb{P}^k(\omega_c)$
- $\mathcal{F}_n = \mathcal{F}(u_h^c, u_h^v, \mathbf{n})$ **numerical flux**

# Numerical example: solid body rotation

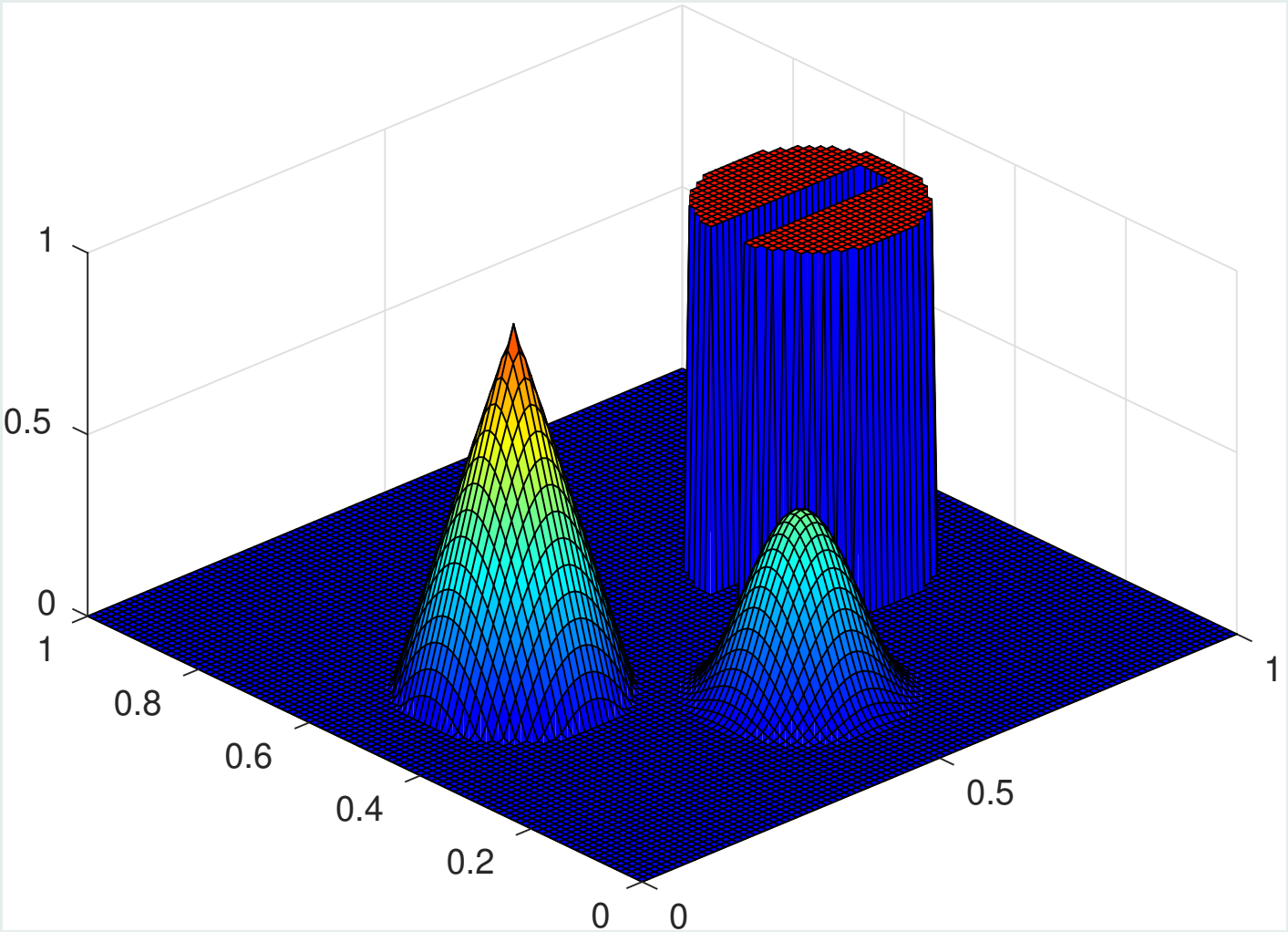


Figure: Rotation of composite signal: initial solution

# Roughly constant number of degrees of freedom $\sim$ **5 100 DoF**

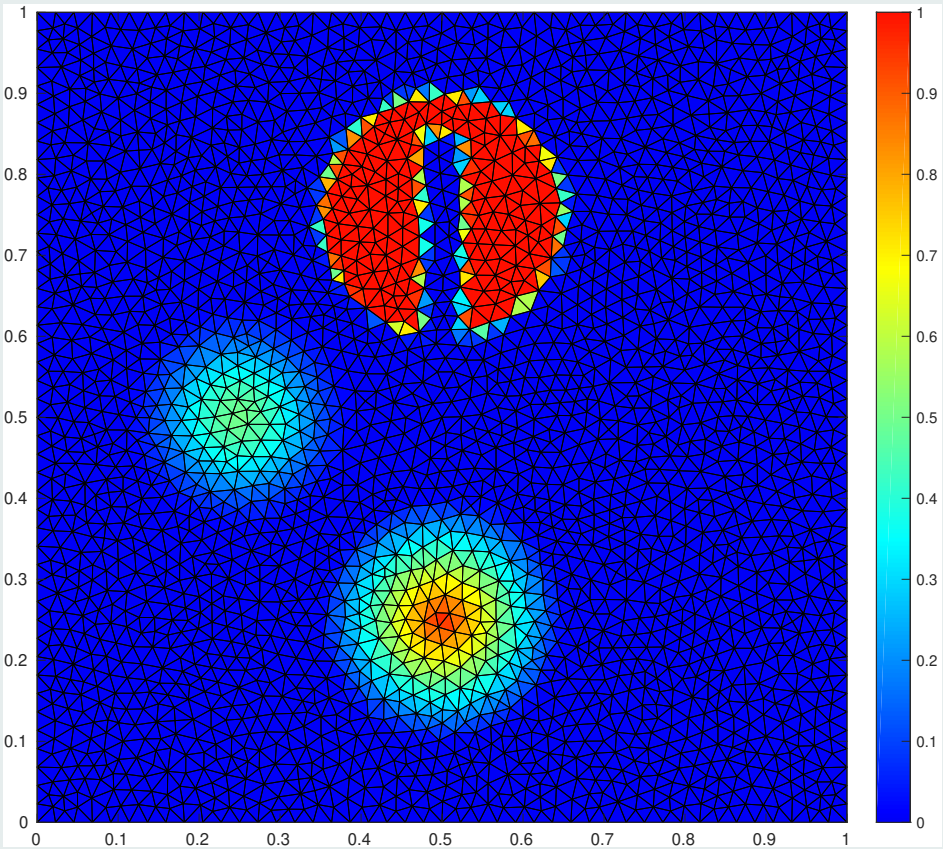


(a) Initial solution

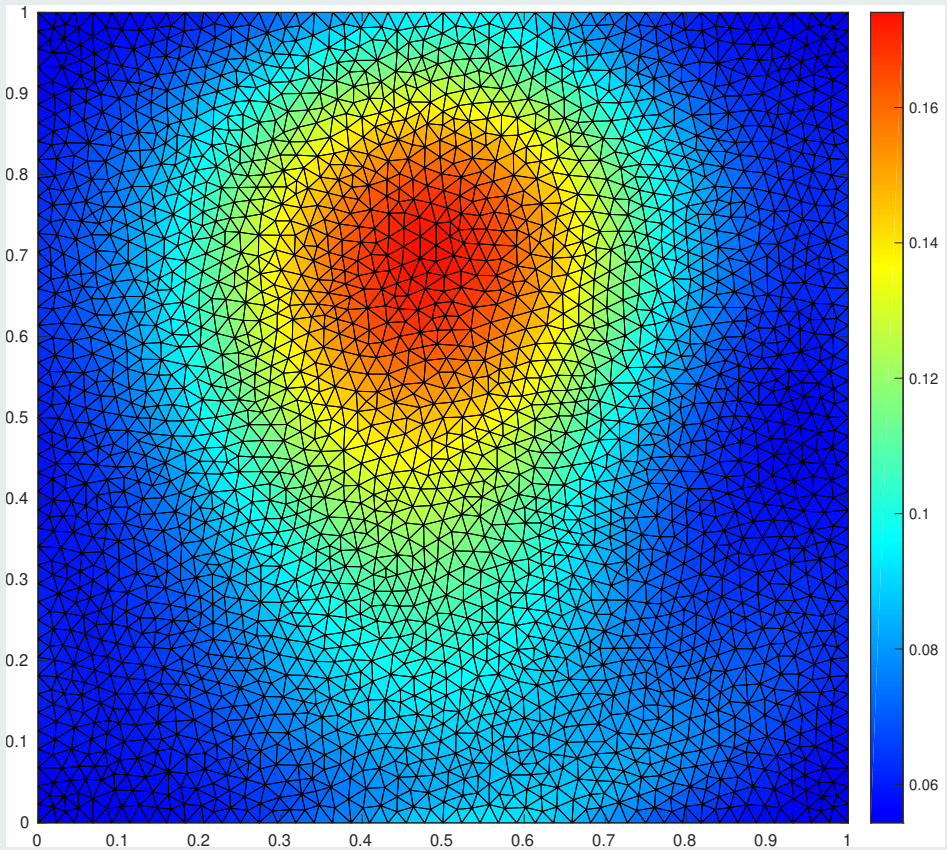


(b) Solution after one rotation

Figure: Rotation of composite signal: 1st-order on 5154 cells

# Roughly constant number of degrees of freedom $\sim$ **5 100 DoF**

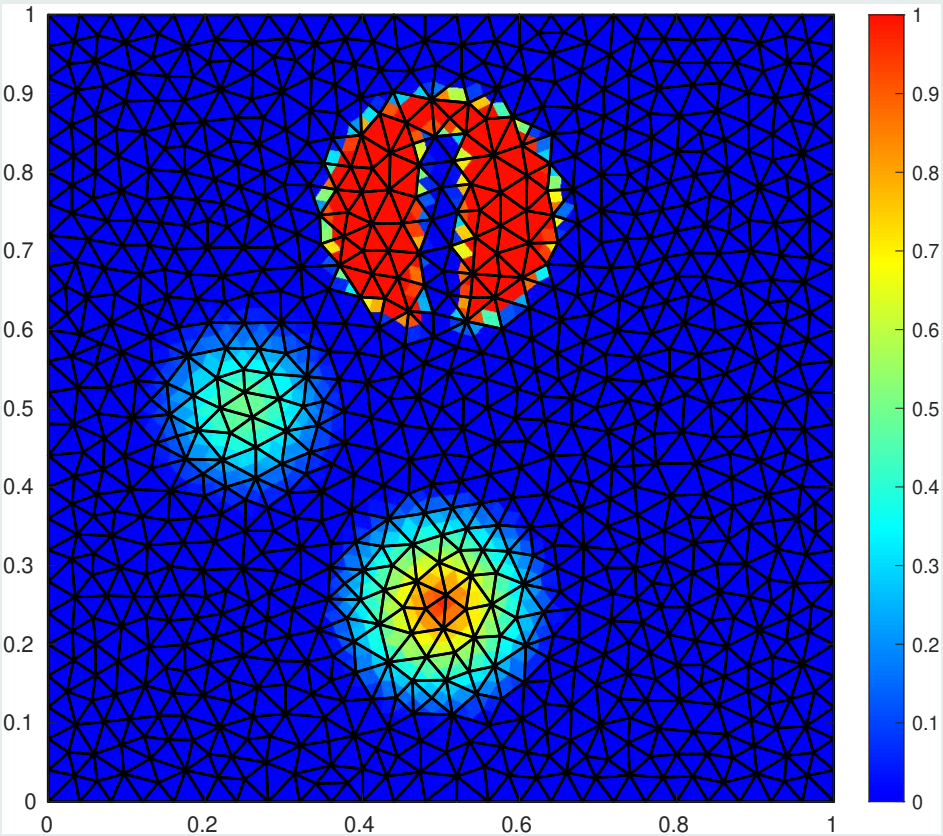


(c) Initial solution

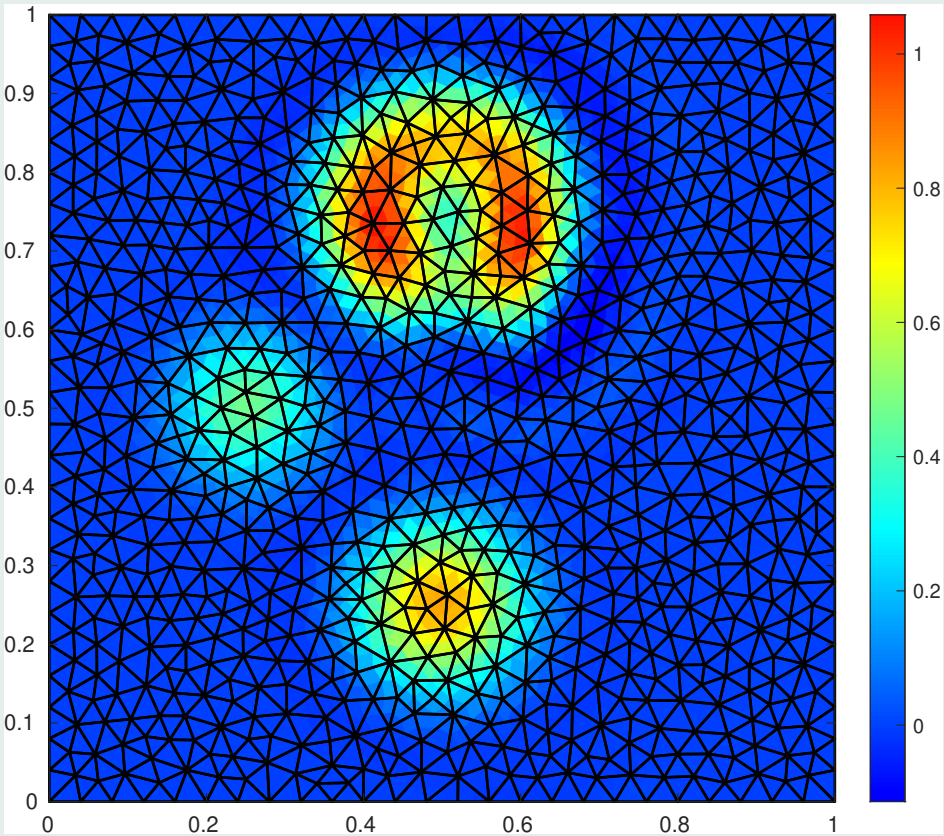


(d) Solution after one rotation

Figure: Rotation of composite signal: 2nd-order on 1680 cells (5040 DoF)

# Roughly constant number of degrees of freedom $\sim$ **5 100 DoF**

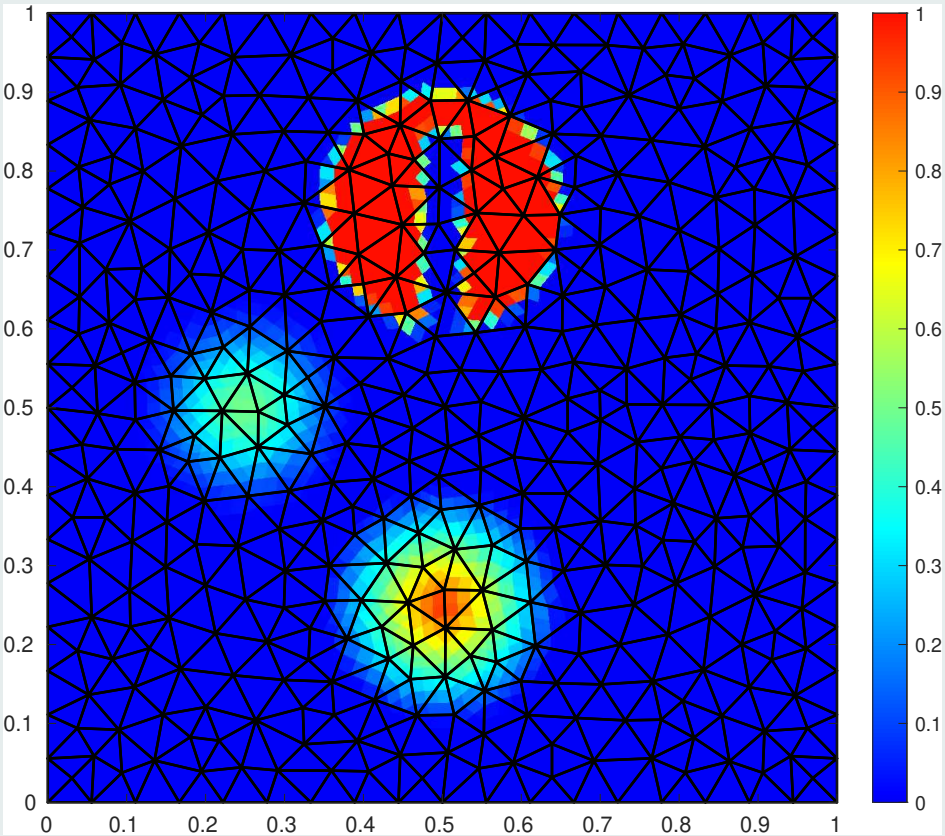


(e) Initial solution

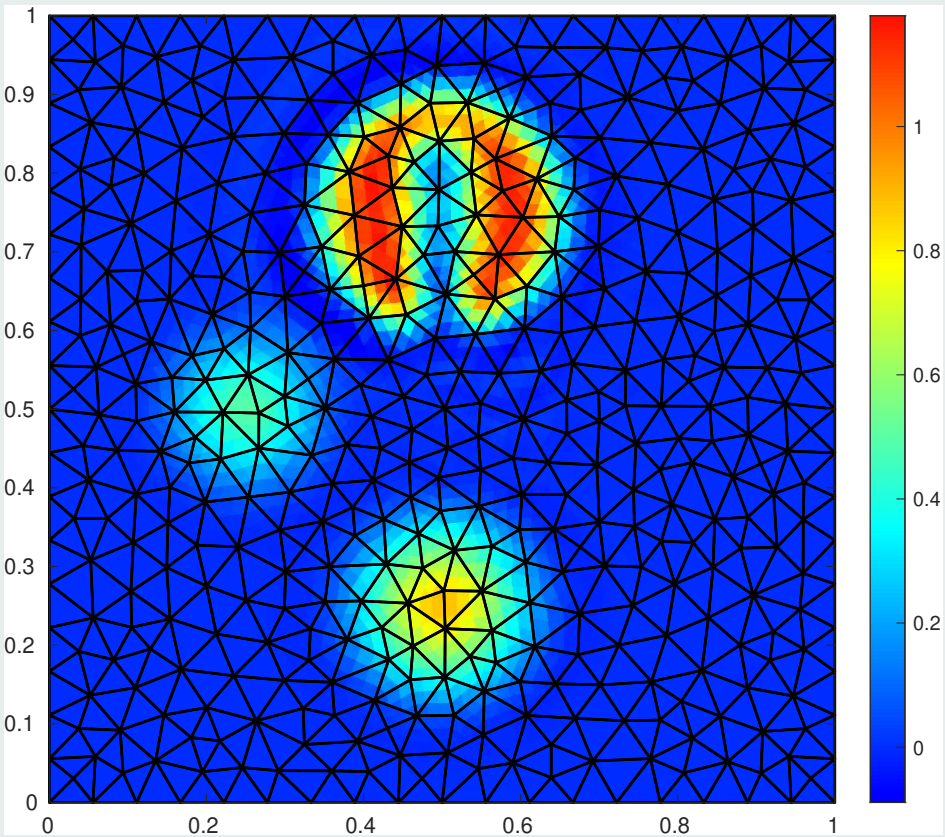


(f) Solution after one rotation

Figure: Rotation of composite signal: 3rd-order on 874 cells (5244 DoF)

# Roughly constant number of degrees of freedom $\sim$ **5 100 DoF**

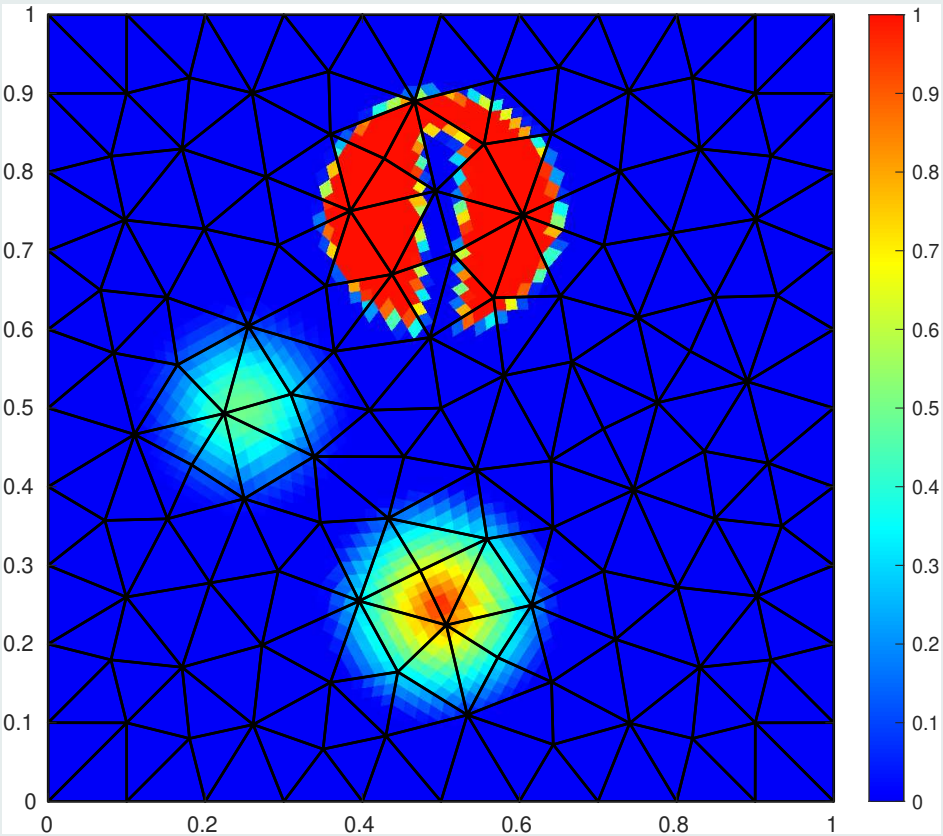


(g) Initial solution

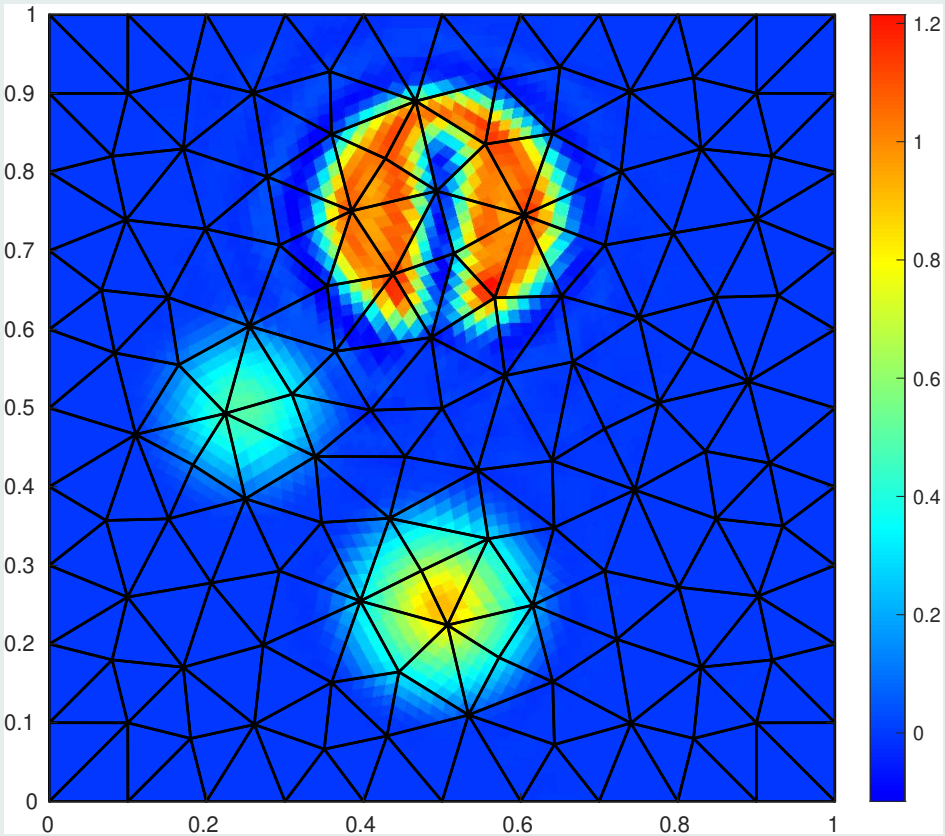


(h) Solution after one rotation

Figure: Rotation of composite signal: 6th-order on 242 cells (5082 DoF)

# Subcell resolution of DG scheme $\sim$ 5 100 DoF

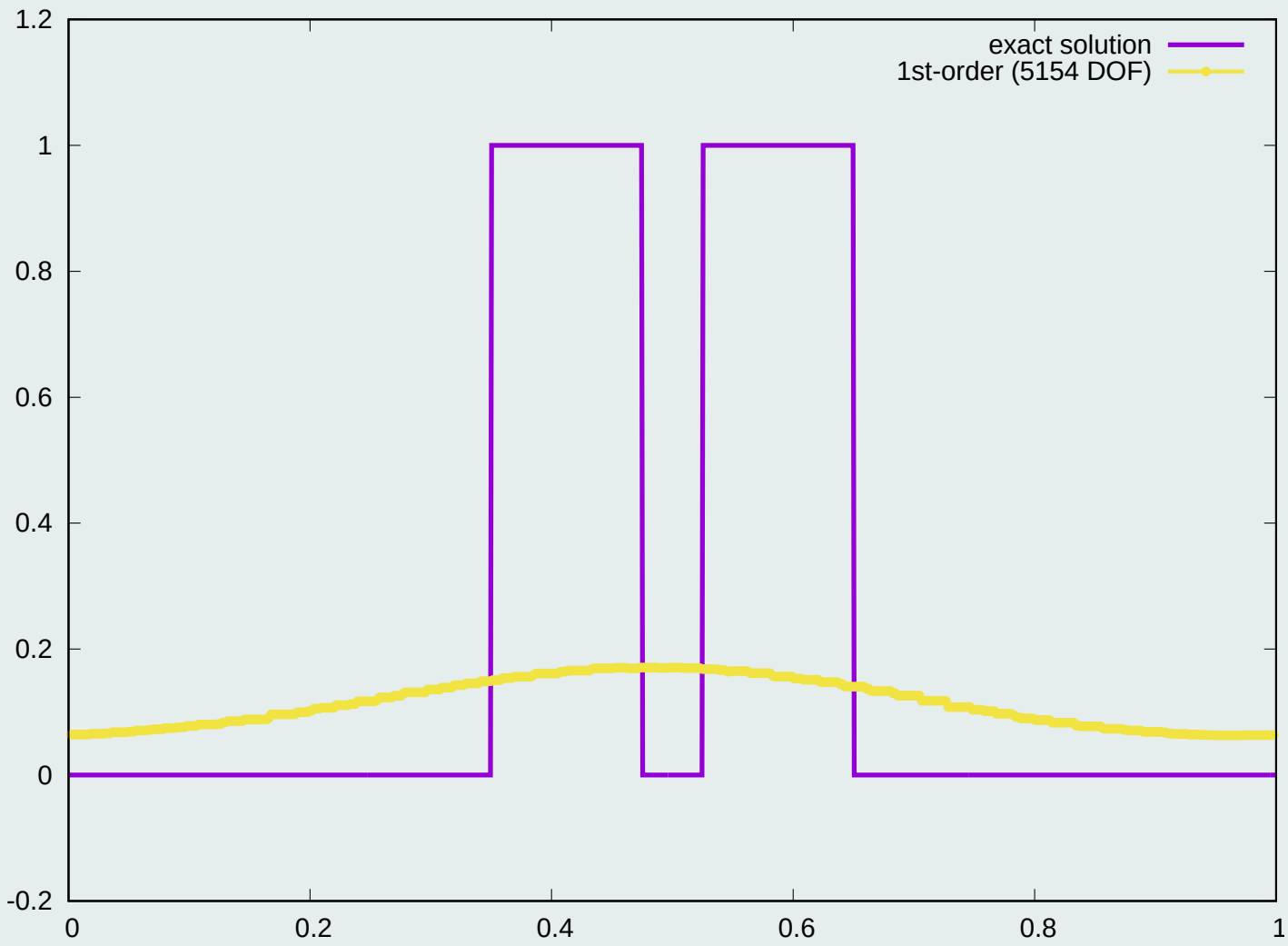


Figure: Rotation of composite signal after one period: profiles for $y = 0.75$

# Subcell resolution of DG scheme $\sim$ 5 100 DoF

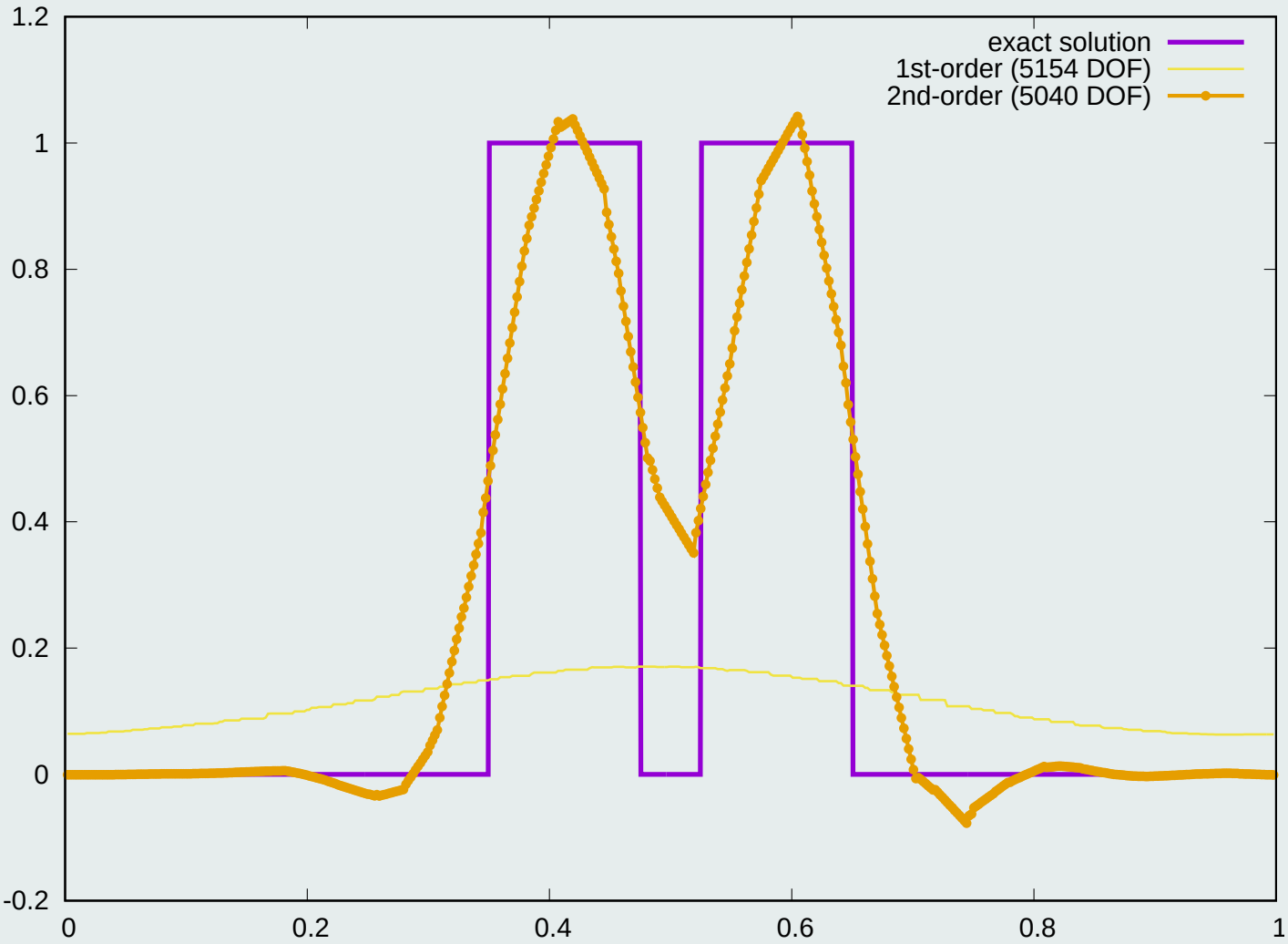


Figure: Rotation of composite signal after one period: profiles for $y = 0.75$

# Subcell resolution of DG scheme $\sim$ 5 100 DoF

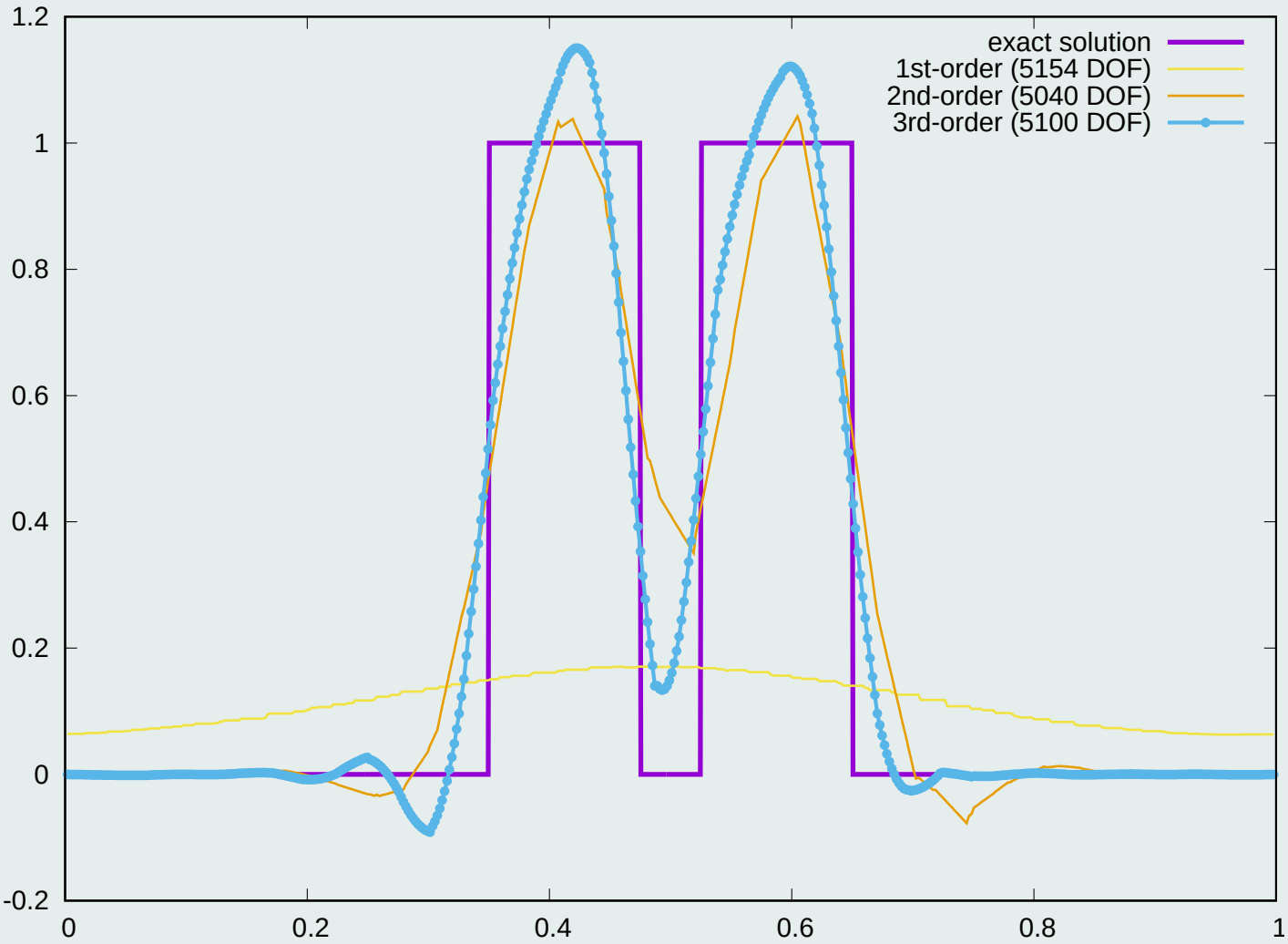


Figure: Rotation of composite signal after one period: profiles for $y = 0.75$

# Subcell resolution of DG scheme $\sim$ 5 100 DoF

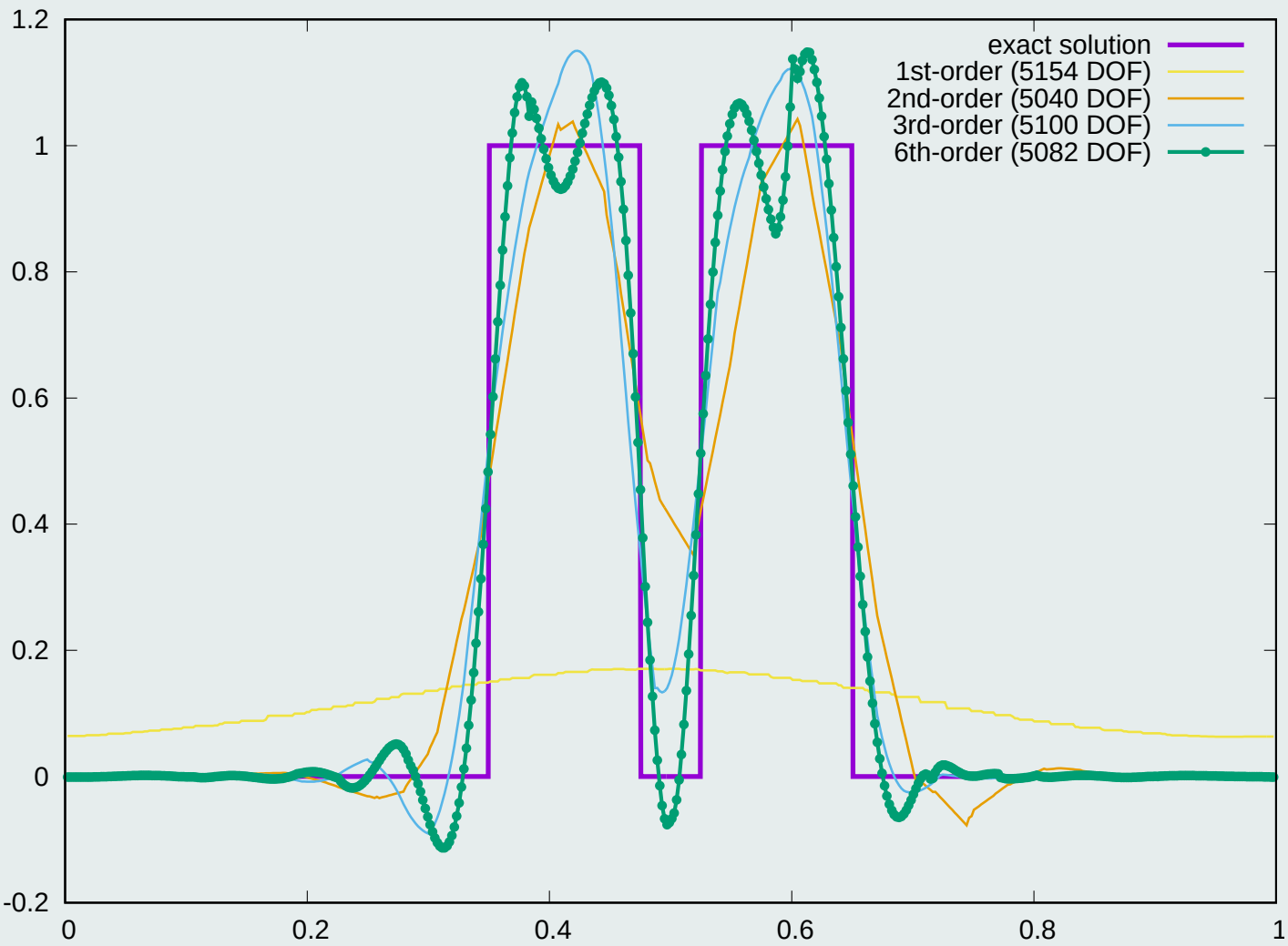


Figure: Rotation of composite signal after one period: profiles for $y = 0.75$

# Spurious oscillations, aliasing and non-entropic behavior

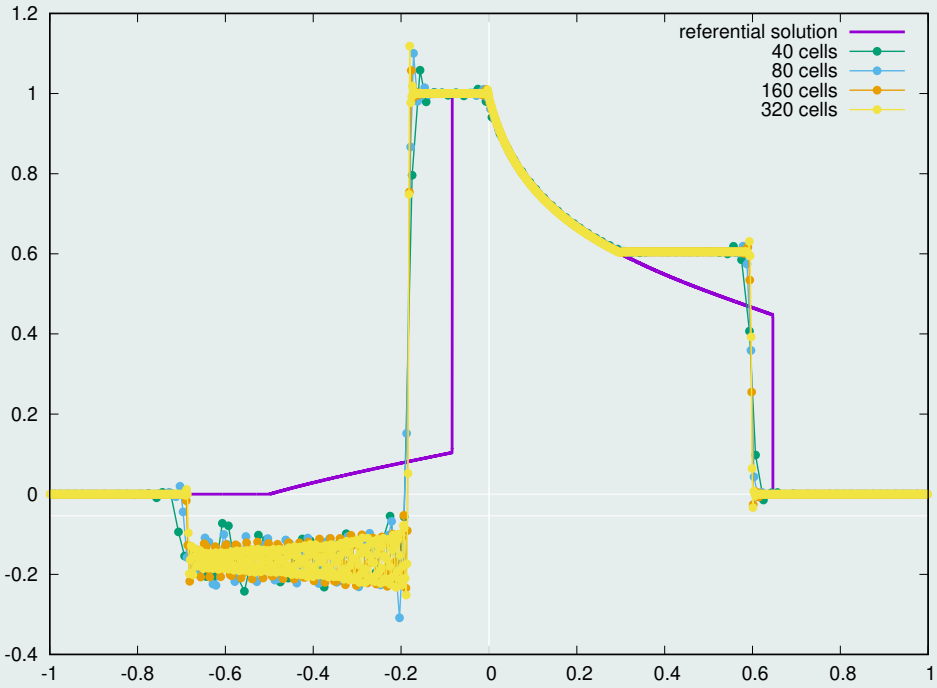


(a) Non-entropic behavior

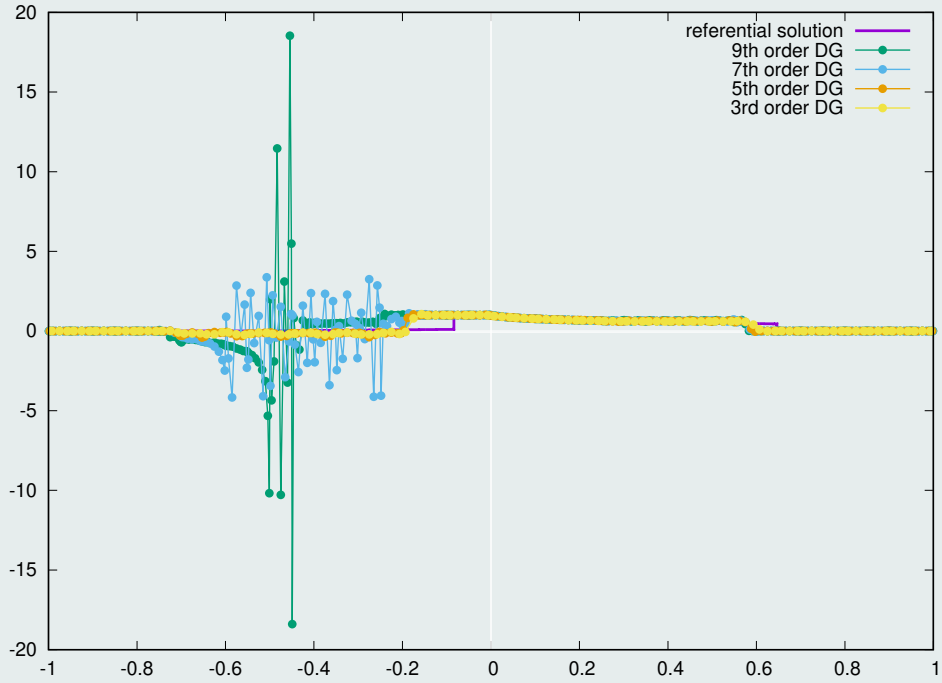


(b) Aliasing phenomenon

Figure : DG solutions for the Buckley non-convex flux case

## Gibbs phenomenon and non-admissible solution

- High-order schemes leads to spurious oscillations near discontinuities
- Non-admissible solution potentially leading to a crash
- Vast literature of how prevent this phenomenon to happen:

$$\Longrightarrow \quad \textit{a priori} \text{ and } \textit{a posteriori} \text{ limitations}$$

## *A priori* limitation

- Artificial viscosity
- Slope/moment/hierarchical limiter
- ENO/WENO limiter
- Flux limiter and FCT schemes
- **Monolithic HO/LO schemes**

## *A posteriori* limitation

- MOOD (“Multi-dimensional Optimal Order Detection”)
- A posteriori subcell correction

## Admissible numerical solution

- Maximum principle / positivity preserving
- Limit the apparition of spurious oscillations
- Ensure a correct entropic behavior

## Preserving high-accuracy and subcell resolution

**Reduce the characteristic length of action**

## Methodology

**Blend, at the subcell scale, high-order DG and 1st-order FV**

**F.V.**, *A Posteriori Correction of High-Order DG Scheme through Subcell Finite Volume Formulation and Flux Reconstruction.* JCP, 2018.

**F.V.**, *Local subcell monolithic DG/FV convex property preserving scheme on unstructured grids and entropy consideration.* JCP, 2024.

# DG as a subcell Finite Volume

- Rewrite DG scheme as a FV-like scheme on a subgrid

## Cell subdivision into $N_S$ subcells $N_S \geq N_k \equiv \#\mathbb{P}^k$

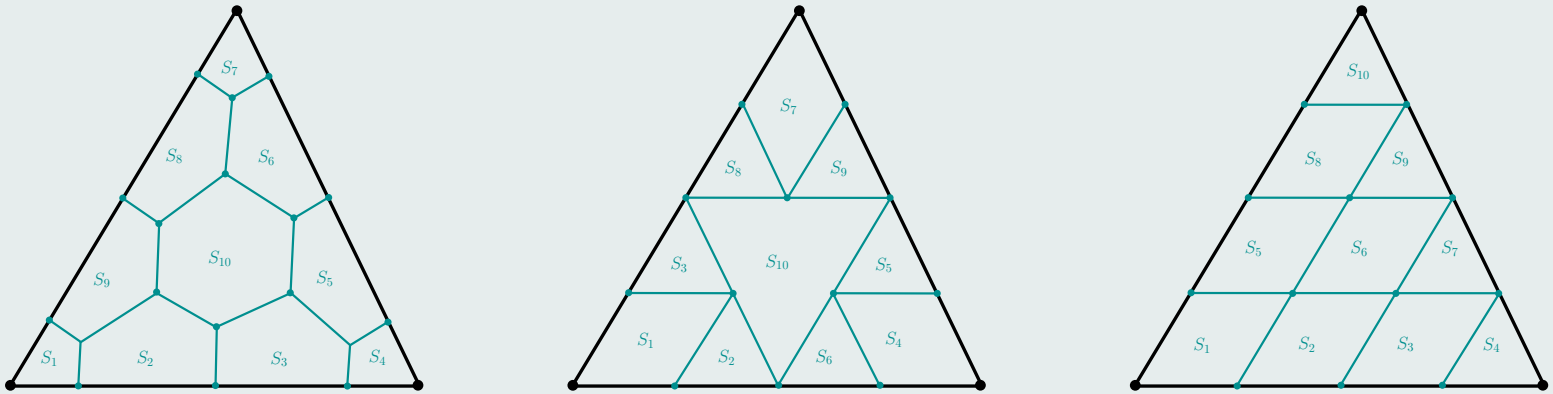


Figure : Examples of $N_s = N_k$ subdivision for $\mathbb{P}^3$ DG scheme on a triangle

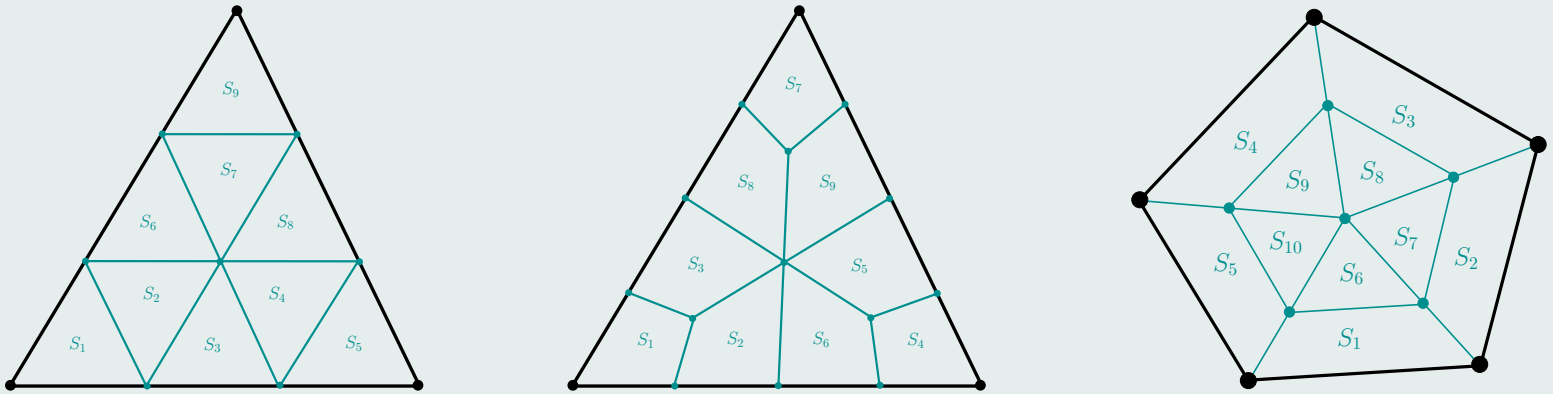


Figure : Examples of $N_S \geq N_k$ subdivision

## DG schemes through residuals

- $$\sum_{m=1}^{N_k} \frac{\mathrm{d}\, u_m^c}{\mathrm{d}t} \int_{\omega_c} \sigma_m \sigma_p \,\mathrm{d}V = \oint_{\omega_c} \mathbf{F}(u_h^c) \cdot \nabla_x \sigma_p \,\mathrm{d}V - \oint_{\partial\omega_c} \sigma_p \,\mathcal{F}_n \,\mathrm{d}S, \quad \forall\, p \in [\![1, N_k]\!]$$

$$\Longrightarrow \qquad \boxed{M_c \frac{\mathrm{d}\, \mathrm{U}_c}{\mathrm{d}t} = \Phi_c}$$

- $(\mathrm{U}_c)_m = u_m^c$ — Solution moments
- $(M_c)_{mp} = \displaystyle\int_{\omega_c} \sigma_m \sigma_p \,\mathrm{d}V$ — Mass matrix
- $(\Phi_c)_m = \displaystyle\oint_{\omega_c} \mathbf{F}(u_h^c) \cdot \nabla_x \sigma_m \,\mathrm{d}V - \oint_{\partial\omega_c} \sigma_m \,\mathcal{F}_n \,\mathrm{d}S$ — DG residuals

## Subdivision and definition

- $\omega_c$ is subdivided into $N_s$ subcells $S_m^c$
- Let us define $\overline{\psi}_m^c = \dfrac{1}{|S_m^c|} \displaystyle\int_{S_m^c} \psi \,\mathrm{d}V$ the subcell mean value

## Submean values

- $\overline{u}_m^c = \dfrac{1}{|S_m^c|} \displaystyle\sum_{q=1}^{N_k} u_q^c \int_{S_m^c} \sigma_q \, \mathrm{d}V \quad \Longrightarrow \quad \boxed{\overline{\mathrm{U}}_c = P_c \, \mathrm{U}_c}$
- $(\overline{\mathrm{U}}_c)_m = \overline{u}_m^c$ Submean values
- $(P_c)_{mp} = \dfrac{1}{|S_m^c|} \displaystyle\int_{S_m^c} \sigma_p \, \mathrm{d}V$ Projection matrix

$$\Longrightarrow \quad \boxed{\frac{\mathrm{d}\,\overline{\mathrm{U}}_c}{\mathrm{d}t} = P_c \, M_c^{-1} \, \Phi_c}$$

## Admissibility of the cell sub-partition into subcells

- $P_c^{\mathrm{t}} P_c$ **has to be non-singular**

$$\Longrightarrow \quad \boxed{\mathrm{U}_c = (P_c^{\mathrm{t}} P_c)^{-1} P_c^{\mathrm{t}} \, \overline{\mathrm{U}}_c}$$ Least square procedure

- If $N_s = N_k$, $\overline{\mathrm{U}}_c = P_c \, \mathrm{U}_c \iff \mathrm{U}_c = P_c^{-1} \overline{\mathrm{U}}_c$

# Subcell Finite Volume: reconstructed fluxes

- Let us introduce the **reconstructed fluxes**

$$\boxed{\frac{\mathrm{d}\,\overline{u}_m^c}{\mathrm{d}t} = -\frac{1}{|S_m^c|}\sum_{S_p^v \in \mathcal{V}_m^c} l_{mp}\,\widehat{F_{pm}}}$$

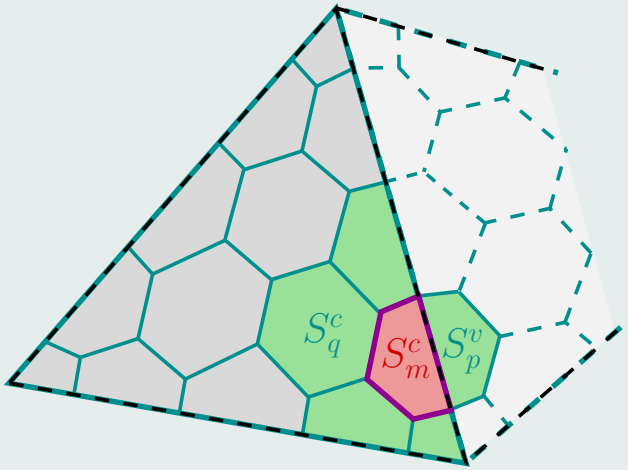


- $\mathcal{V}_m^c$ the set of face neighboring subcells of $S_m^c$
- We impose that on the boundary of cell $\omega_c$, so for $S_p^v \notin \omega_c$

$$\boxed{l_{mp}\,\widehat{F_{pm}} = \oint_{f_{mp}^c} \mathcal{F}_n\,\mathrm{d}S \equiv \oint_{f_{mp}^c} \mathcal{F}\left(u_h^c,\, u_h^v,\, \boldsymbol{n}_{mp}^c\right)\,\mathrm{d}S}$$

- $\widetilde{\mathcal{V}_m^c}$ the set of face neighboring subcells of $S_m^c$ belonging to $\omega_c$
- Let $A_c$ be the adjacency matrix such that

$$(A_c)_{mp} = \begin{cases} 1 & \text{if } S_p^v \in \widetilde{\mathcal{V}_m^c} \text{ with } m < p, \\ -1 & \text{if } S_p^v \in \widetilde{\mathcal{V}_m^c} \text{ with } m > p, \\ 0 & \text{if } S_p^v \notin \widetilde{\mathcal{V}_m^c}. \end{cases}$$

## Subcell Finite Volume: reconstructed fluxes

- Let us introduce $D_c = \text{diag}\left(|S_1^c|, \ldots, |S_{N_k}^c|\right)$ and $(\mathrm{B}_c)_m = \displaystyle\int_{\partial S_m^c \cap \partial\omega_c} \mathcal{F}_n \, \mathrm{d}S$
- Let $\widehat{\mathrm{F}_c}$ be the vector containing all the interior faces reconstructed fluxes

$$\boxed{-A_c \, \widehat{\mathrm{F}_c} = D_c \, P_c \, M_c^{-1} \, \Phi_c + \mathrm{B}_c}$$

## Graph Laplacian technique

- $A_c \in \mathcal{M}_{N_s \times N_f^c}$ with $N_f^c$ the number of interior faces
- $(L_c)_{mp} := \left(A_c \, A_c^{\mathrm{t}}\right)_{mp} = \begin{cases} |\widetilde{\mathcal{V}_m^c}| & \text{if } m = p, \\ -1 & \text{if } S_p^v \in \widetilde{\mathcal{V}_m^c}, \\ 0 & \text{otherwise.} \end{cases}$
- $L_c \mathbf{1} = \mathbf{0}$ where $\mathbf{1} = (1, \ldots, 1)^{\mathrm{t}} \in \mathbb{R}^{N_s}$
- $\Pi = \frac{1}{N_s} \, (\mathbf{1} \otimes \mathbf{1}) \in \mathcal{M}_{N_s}$

## Graph Laplacian technique

- Let $\mathcal{L}_c^{-1}$ be the pseudo-inverse of $L_c$ such that

$$\mathcal{L}_c^{-1} = (L_c + \lambda\,\Pi)^{-1} - \frac{1}{\lambda}\,\Pi \qquad \forall\,\lambda \neq 0$$

- Then, $\widehat{\mathrm{F}_c}$ is uniquely defined as following

$$\boxed{\widehat{\mathrm{F}_c} = -A_c^{\mathrm{t}}\,\mathcal{L}_c^{-1}\left(D_c\,P_c\,M_c^{-1}\,\Phi_c + \mathrm{B}_c\right)}$$

- **The only terms depending on the time are $\Phi_c$ and $\mathrm{B}_c$**

- Equivalently, the polynomial solution governing equation is given by

$$\frac{\mathrm{d}\,\mathrm{U}_c}{\mathrm{d}t} = -P_c^{-1}\,D_c^{-1}\left(A_c\,\widehat{\mathrm{F}_c} + \mathrm{B}_c\right)$$

## remark

- This unique solution does exit since $\left(D_c\,P_c\,M_c^{-1}\,\Phi_c + \mathrm{B}_c\right)\cdot\mathbf{1} = 0$

# Blending low and high order fluxes

- Each face $f_{mp}^c$ of each subcell $S_m^c$ will be assigned two fluxes
-
$$\widetilde{F_{mp}} = \mathcal{F}_{mp}^{\text{FV}} + \underbrace{\theta_{mp}}_{\in [0,1]} \underbrace{\left(\widehat{F_{mp}} - \mathcal{F}_{mp}^{\text{FV}}\right)}_{\Delta F_{mp}}$$

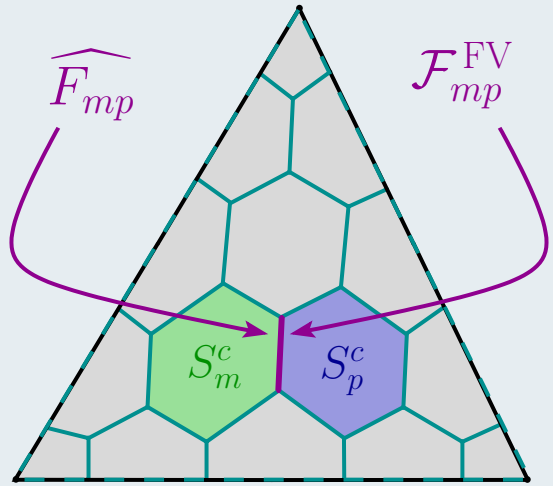


- $\mathcal{F}_{mp}^{\text{FV}} := \mathcal{F}\left(\overline{u}_m^c, \overline{u}_p^v, \boldsymbol{n}_{mp}\right)$ first-order subcell numerical flux
- $\widehat{F_{mp}}$ high-order DG reconstructed flux
- **The local subcell monolithic DG/FV then writes as follows**

$$\frac{\mathrm{d}\,\overline{u}_m^c}{\mathrm{d}t} = -\frac{1}{|S_m^c|} \sum_{S_p^v \in \mathcal{V}_m^c} l_{mp}\, \widetilde{F_{mp}}$$

## Numerical flux

- $\mathcal{F}(u^-, u^+, \boldsymbol{n}) = \dfrac{\big(\boldsymbol{F}(u^-) + \boldsymbol{F}(u^+)\big)}{2} \cdot \boldsymbol{n} - \dfrac{\gamma(u^-, u^+, \boldsymbol{n})}{2}(u^+ - u^-)$
- $\gamma(u^-, u^+, \boldsymbol{n}) \geq \max\limits_{w \in \mathrm{I}(u^-, u^+)} \big(|\boldsymbol{F}'(w) \cdot \boldsymbol{n}|\big)$
- **In the system case, we make use of either Rusanov, HLL, HLL-C, ...**

## Reformulation of the monolithic subcell scheme

- $$\overline{u}_m^{c,n+1} = \overline{u}_m^{c,n} - \frac{\Delta t}{|S_m^c|}\left(\sum_{S_p^v \in \mathcal{V}_m^c} l_{mp}\, \widetilde{F_{mp}} \pm \sum_{S_p^v \in \mathcal{V}_m^c} l_{mp}\, \gamma_{mp}\, \overline{u}_m^{c,n} + \boldsymbol{F}(\overline{u}_m^{c,n}) \cdot \sum_{S_p^v \in \mathcal{V}_m^c} l_{mp}\, \boldsymbol{n}_{mp}\right)$$

$$= \left(1 - \frac{\Delta t}{|S_m^c|} \sum_{S_p^v \in \mathcal{V}_m^c} l_{mp}\, \gamma_{mp}\right) \overline{u}_m^{c,n} + \frac{\Delta t}{|S_m^c|} \sum_{S_p^v \in \mathcal{V}_m^c} l_{mp}\, \gamma_{mp}\, \widetilde{u_{mp}}^-$$

- $$\widetilde{u_{mp}}^{\pm} = \underbrace{\frac{\overline{u}_m^{c,n} + \overline{u}_p^{v,n}}{2} - \frac{\big(\boldsymbol{F}(\overline{u}_p^{v,n}) - \boldsymbol{F}(\overline{u}_m^{c,n})\big) \cdot \boldsymbol{n}_{mp}}{2\,\gamma_{mp}}}_{u_{mp}^{*,\,\mathrm{FV}}} \pm \theta_{mp} \frac{\Delta F_{mp}}{\gamma_{mp}}$$

# Admissible solution — Find the correct $\theta_{mp}$

- $G$ a convex admissible set where the solution has to remain in
  - $G = \left\{ u_0 \in [\alpha, \beta] \implies u \in [\alpha, \beta] \right\}$ SCL
  - $G = \left\{ u = \begin{pmatrix} \rho \\ \boldsymbol{q} \\ E \end{pmatrix}, \quad \rho > 0,\ p(u) > 0 \right\}$ Euler
- **A sufficient condition to ensure $\overline{u}_m^{c,n+1} \in G$ is that**

$$\forall\, S_p^v \in \mathcal{V}_m^c, \qquad \widetilde{u_{mp}}^{\pm} = u_{mp}^{*,\mathrm{FV}} \pm \theta_{mp} \frac{\Delta F_{mp}}{\gamma_{mp}} \in G$$

- We want to prevent to code from crashing (apparition of NaN, . . . )
- We want to prevent the apparition of spurious oscillations
- ***We want to ensure discrete entropy inequalities (?)***
- We apply a local blending coefficients smoothening to avoid too stiff transition from high to low orders

# *Séminaire* **SISMA**

## *06/02/2025*

## Global maximum principle

$$\overline{u}_m^{c,n+1} \in [\alpha,\ \beta]$$

$$\theta_{mp} \leq \min\left(1,\ \left|\frac{\gamma_{mp}}{\Delta F_{mp}}\right| \min\left(\beta - u_{mp}^{*,\mathrm{FV}},\ u_{mp}^{*,\mathrm{FV}} - \alpha\right)\right)$$

## Local maximum principle

$$\overline{u}_m^{c,n+1} \in [\alpha_m^c,\ \beta_m^c]$$

- $\alpha_m^c := \min_{S_q^w \in \mathcal{N}(S_m^c)} \left(\overline{u}_q^{w,n}\right)$ and $\beta_m^c := \max_{S_q^w \in \mathcal{N}(S_m^c)} \left(\overline{u}_q^{w,n}\right)$

$$\theta_{mp} \leq \min\left(1,\ \left|\frac{\gamma_{mp}}{\Delta F_{mp}}\right| \begin{cases} \min\left(\beta_p^v - u_{mp}^{*,\mathrm{FV}},\ u_{mp}^{*,\mathrm{FV}} - \alpha_m^c\right) & \text{if } \Delta F_{mp} > 0 \\ \min\left(\beta_m^c - u_{mp}^{*,\mathrm{FV}},\ u_{mp}^{*,\mathrm{FV}} - \alpha_p^v\right) & \text{if } \Delta F_{mp} < 0 \end{cases}\right)$$

- The wider set $\mathcal{N}(S_m^c)$ is, the softer this local maximum principle will be
- **Smooth extrema relaxation to preserve accuracy**

# Burgers equation

$u_0(x, y) = \sin(2\pi(x + y))$

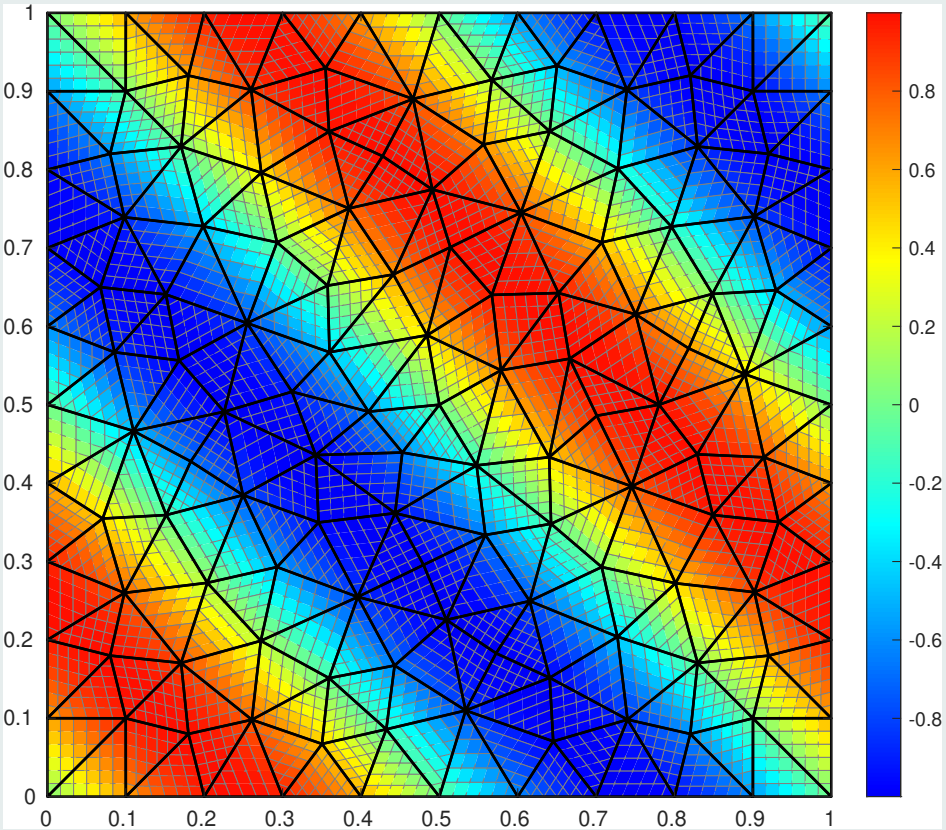


(a) Solution submean values

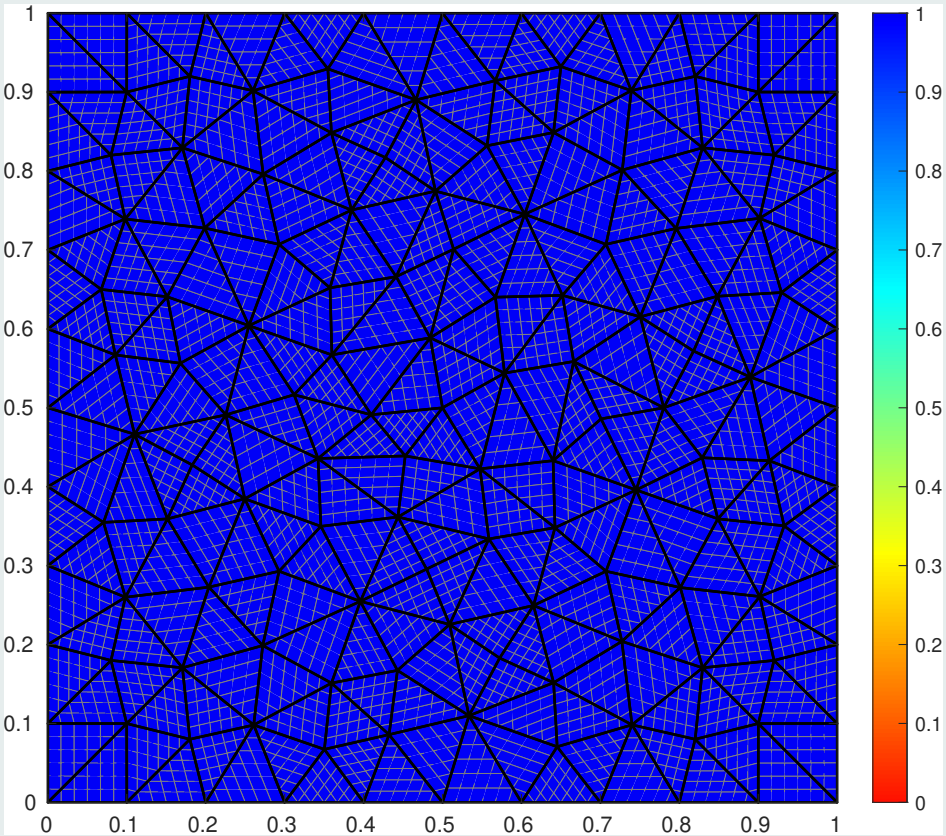


(b) Blending coefficients

Figure: $\mathbb{P}^5$-DG/FV scheme with GMP and relaxed-LMP on 242 cells

# KPP non-convex flux problem

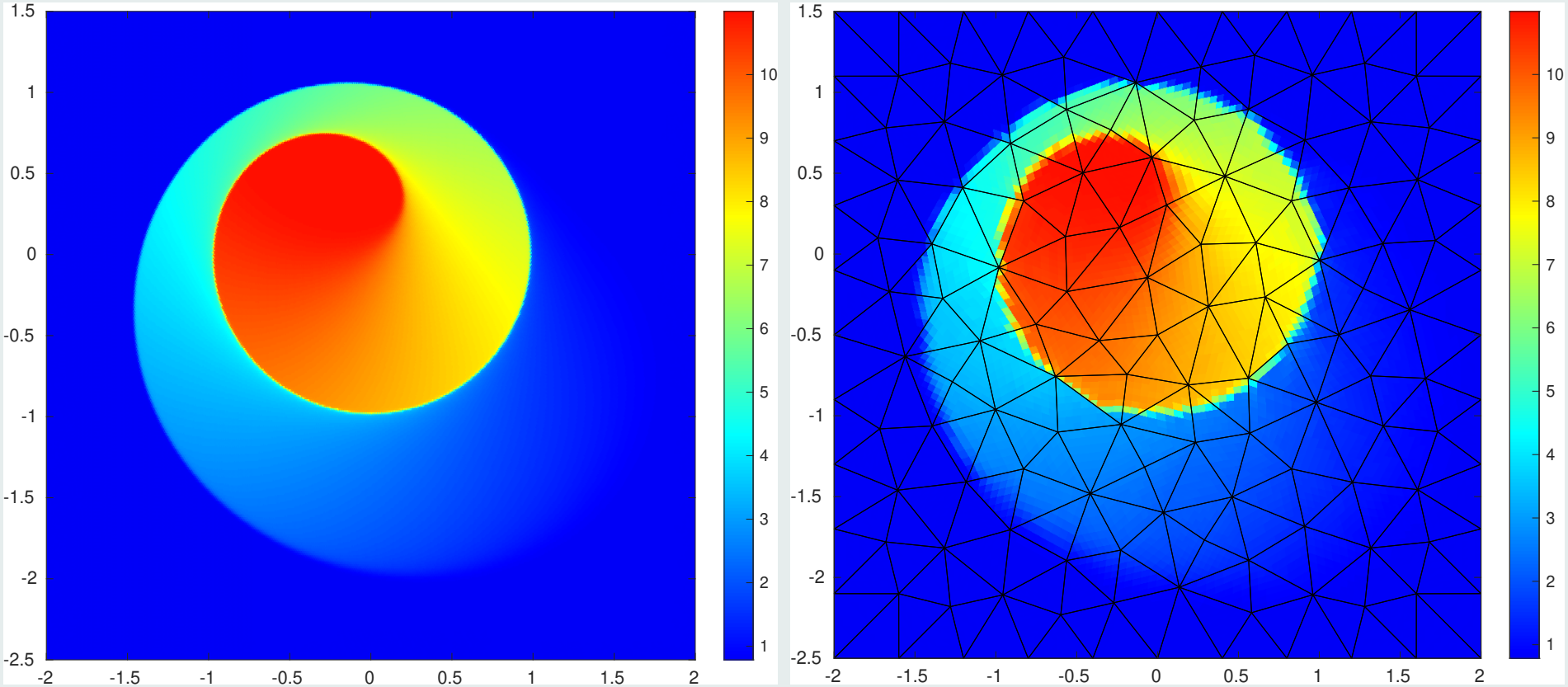


(a) $1^{\text{th}}$-order FV on 209184 cells

(b) $\mathbb{P}^7$-DG/FV on 272 cells

Figure: $\mathbb{P}^7$-DG/FV scheme with GMP and relaxed-LMP

## Non-linear Euler compressible gas dynamics equations

- $\partial_t \boldsymbol{V} + \nabla_x \cdot \boldsymbol{F}(\boldsymbol{V}) = \boldsymbol{0}$
- $\boldsymbol{V} = \begin{pmatrix} \rho \\ \boldsymbol{q} \\ E \end{pmatrix}$ conservative variables
- $\boldsymbol{F}(\boldsymbol{V}) = \begin{pmatrix} \boldsymbol{q} \\ \dfrac{\boldsymbol{q} \otimes \boldsymbol{q}}{\rho} + p\, I_d \\ (E+p)\dfrac{\boldsymbol{q}}{\rho} \end{pmatrix}$ flux function
- $p := p(\boldsymbol{V}) = (\gamma - 1)\left(E - \frac{1}{2}\frac{\|\boldsymbol{q}\|^2}{\rho}\right)$ equation of state

## Monolithic subcell DG/FV scheme property

- Positivity of the density and internal energy, at the subcell scale

## Definitions

- $\widetilde{\boldsymbol{F}_{mp}} := \boldsymbol{\mathcal{F}}^{\mathrm{FV}}_{mp} + \Theta_{mp} \underbrace{\left(\widehat{\boldsymbol{F}_{mp}} - \boldsymbol{\mathcal{F}}^{\mathrm{FV}}_{mp}\right)}_{\Delta \boldsymbol{F}_{mp}}$ convex blended flux
- $\Theta_{mp} = \begin{pmatrix} \theta^{\rho}_{mp} & \mathbf{0} & 0 \\ \mathbf{0} & \boldsymbol{\theta}^{\boldsymbol{q}}_{mp} & \mathbf{0} \\ 0 & \mathbf{0} & \theta^{E}_{mp} \end{pmatrix}$
- $\boldsymbol{\mathcal{F}}^{\mathrm{FV}}_{mp} := \boldsymbol{\mathcal{F}}\left(\overline{\boldsymbol{V}}^{c,n}_{m}, \overline{\boldsymbol{V}}^{v,n}_{p}, \boldsymbol{n}_{mp}\right)$ Global L-F, Rusanov, HLL(C), ...

## Positivity of the density

- $\theta^{\rho}_{mp} = \theta^{(1)}_{mp}\, \theta^{(2)}_{mp}$

$$\theta^{(1)}_{mp} \leq \min\left(1, \left|\frac{\gamma_{mp}}{\Delta F^{\rho}_{mp}}\right| \rho^{*,\,\mathrm{FV}}_{mp}\right)$$

# Positivity of the internal energy

- $A_{mp} = \dfrac{1}{(\gamma_{mp})^2}\left(\dfrac{1}{2}\left\|\Delta \boldsymbol{F}^{\boldsymbol{q}}_{mp}\right\|^2 - \theta^{(1)}_{mp}\,\Delta F^{\rho}_{mp}\,\Delta F^{E}_{mp}\right)$
- $B_{mp} = \dfrac{1}{\gamma_{mp}}\left(\boldsymbol{q}^{*,\,\mathrm{FV}}_{mp} \cdot \Delta \boldsymbol{F}^{\boldsymbol{q}}_{mp} - \rho^{*,\,\mathrm{FV}}_{mp}\,\Delta F^{E}_{mp} - \theta^{(1)}_{mp}\,E^{*,\,\mathrm{FV}}_{mp}\,\Delta F^{\rho}_{mp}\right)$
- $M_{mp} = \rho^{*,\,\mathrm{FV}}_{mp}\,E^{*,\,\mathrm{FV}}_{mp} - \frac{1}{2}\left\|\boldsymbol{q}^{*,\,\mathrm{FV}}_{mp}\right\|^2$

$$\theta^{(2)}_{mp} \leq \min\left(1,\ \frac{M_{mp}}{\left|B_{mp}\right| + \max\left(0, A_{mp}\right)}\right)$$

- $\theta^{\rho}_{mp} = \theta^{\rho\,(1)}_{mp}\,\theta^{(2)}_{mp}, \quad \theta^{q^x}_{mp} = \theta^{(2)}_{mp}, \quad \theta^{q^y}_{mp} = \theta^{(2)}_{mp}, \quad \theta^{E}_{mp} = \theta^{(2)}_{mp}$

**A. Rueda-Ramírez, B. Bolm, D. Kuzmin** and **G. Gassner**, *Monolithic Convex Limiting for Legendre-Gauss-Lobatto Discontinuous Galerkin Spectral Element Methods.* Commun. Appl. Math. Comput., 2024.

## LMP

$\overline{v}_m^{c,n+1} \in [\alpha_m^c, \beta_m^c]$

- $v \in \left\{\rho, q^x, q^y, E\right\}$ conservative variable
- $\alpha_m^c := \min\limits_{S_q^w \in \mathcal{N}(S_m^c)} \left(\overline{v}_q^{w,n}, v_{mq}^{*,\mathrm{FV}}\right)$ and $\beta_m^c := \max\limits_{S_q^w \in \mathcal{N}(S_m^c)} \left(\overline{u}_q^{w,n}, v_{mq}^{*,\mathrm{FV}}\right)$

$$\theta_{mp} \leq \min\left(1, \left|\frac{\gamma_{mp}}{\Delta F_{mp}}\right| \begin{cases} \min\left(\beta_p^v - u_{mp}^{*,\mathrm{FV}}, u_{mp}^{*,\mathrm{FV}} - \alpha_m^c\right) & \text{if } \Delta F_{mp} > 0 \\ \min\left(\beta_m^c - u_{mp}^{*,\mathrm{FV}}, u_{mp}^{*,\mathrm{FV}} - \alpha_p^v\right) & \text{if } \Delta F_{mp} < 0 \end{cases}\right)$$

- **Smooth extrema relaxation to preserve accuracy**

# Sod shock tube test case 10 cells

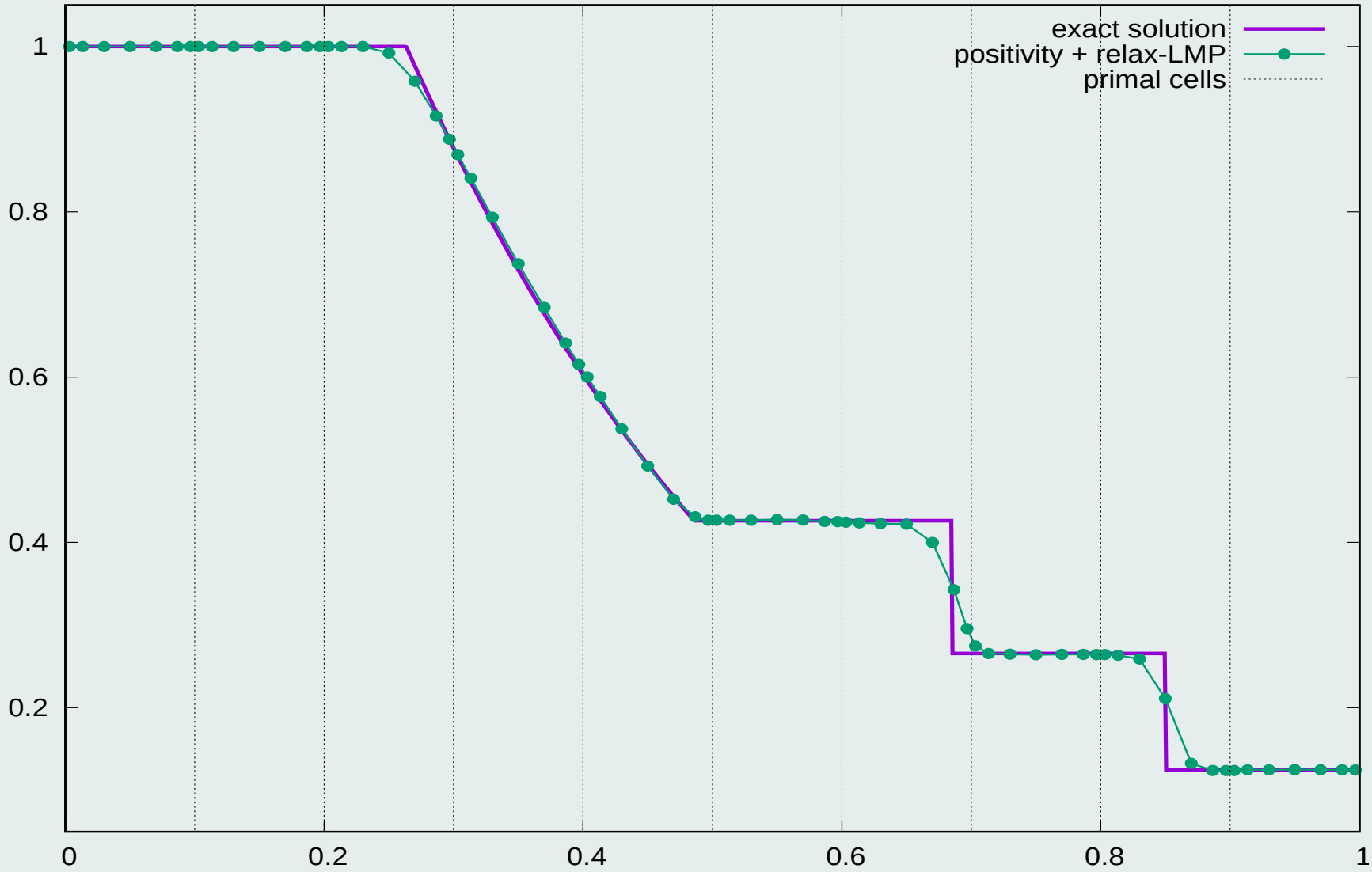


Figure: $\mathbb{P}^6$-DG/FV scheme with GMP and relaxed-LMP: submean values

# Smooth isentropic solution $\rho_0 = 1 + 0.9999999 \sin(2\pi x)$

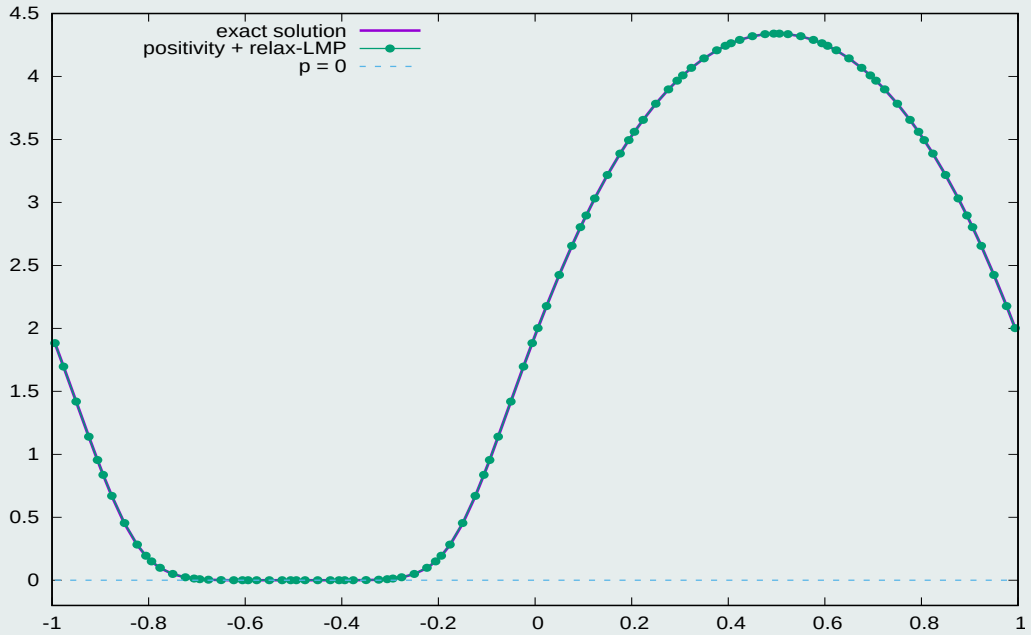


| | $L_1$ | | $L_2$ | | $\theta_{mp}$ | |
|---|---|---|---|---|---|---|
| $h$ | $E^h_{L_1}$ | $q^h_{L_1}$ | $E^h_{L_2}$ | $q^h_{L_2}$ | min. $\theta_{mp}$ | aver. $\theta_{mp}$ |
| $\frac{1}{10}$ | 9.07E-4 | 5.86 | 1.23E-3 | 5.90 | 2.00E-1 | 0.981 |
| $\frac{1}{20}$ | 1.56E-5 | 4.03 | 2.05E-5 | 3.83 | 1.92E-1 | 0.997 |
| $\frac{1}{40}$ | 9.53E-7 | 4.89 | 1.44E-6 | 4.85 | 5.65E-4 | 0.999 |
| $\frac{1}{80}$ | 3.21E-8 | 4.80 | 5.00E-8 | 4.87 | 3.48E-5 | 0.999 |
| $\frac{1}{160}$ | 1.15E-9 | - | 1.71E-9 | - | 1.00 | 1.00 |

Table: Convergence rates of the $\mathbb{P}^4$-DG/FV scheme with positivity and relaxed-LMP

# Sod shock tube problem in cylindrical geometry

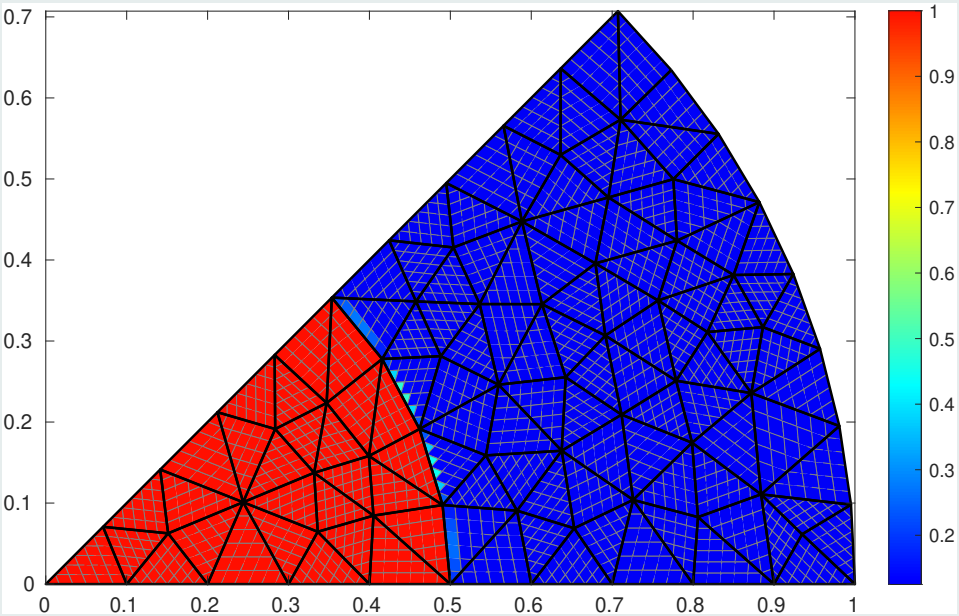


(a) Density map

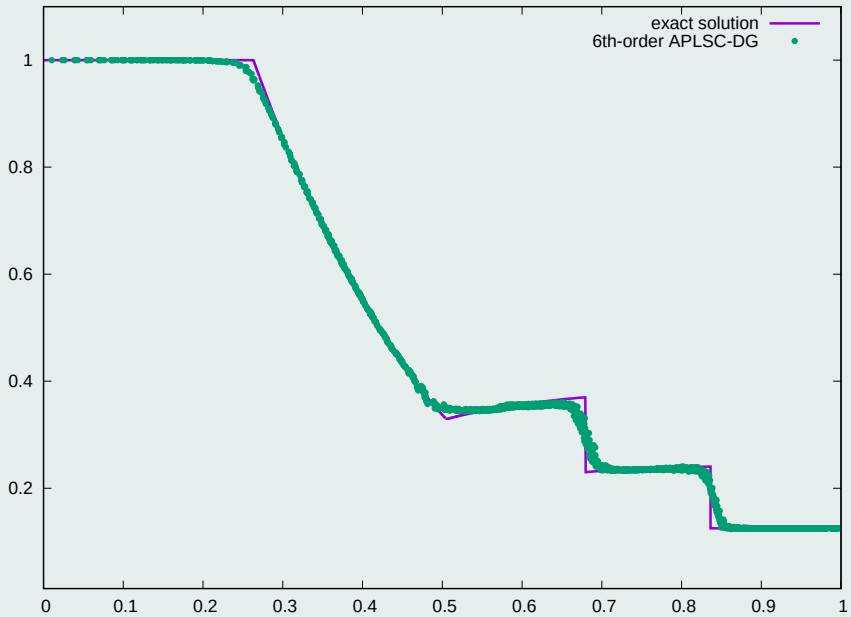


(b) Density profile

Figure: $\mathbb{P}^5$-DG/FV with positivity and relaxed-LMP on a 110 cells mesh

# Sedov point blast problem in cylindrical geometry

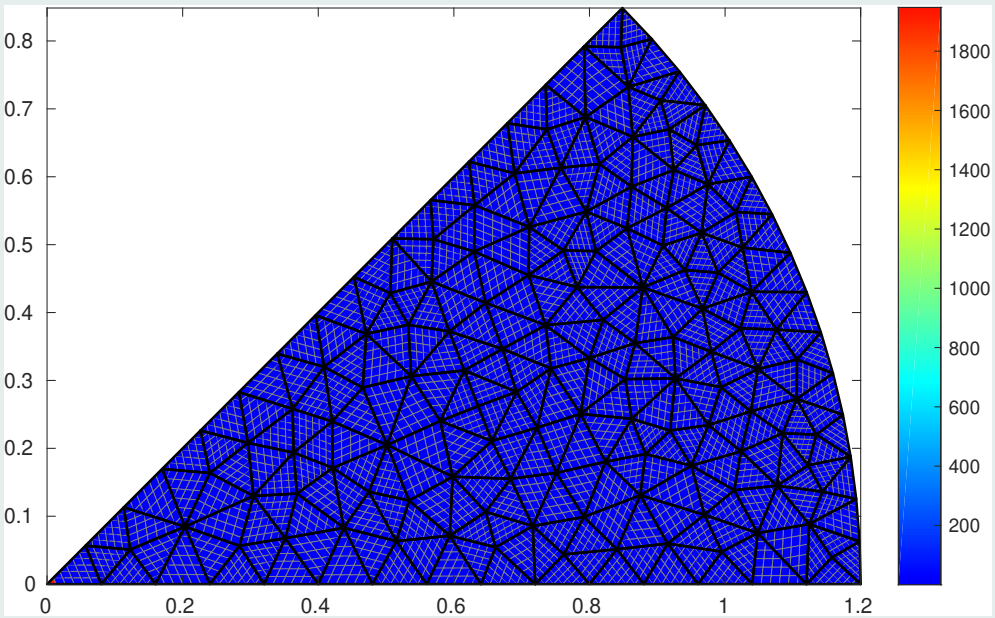


(a) Energy map

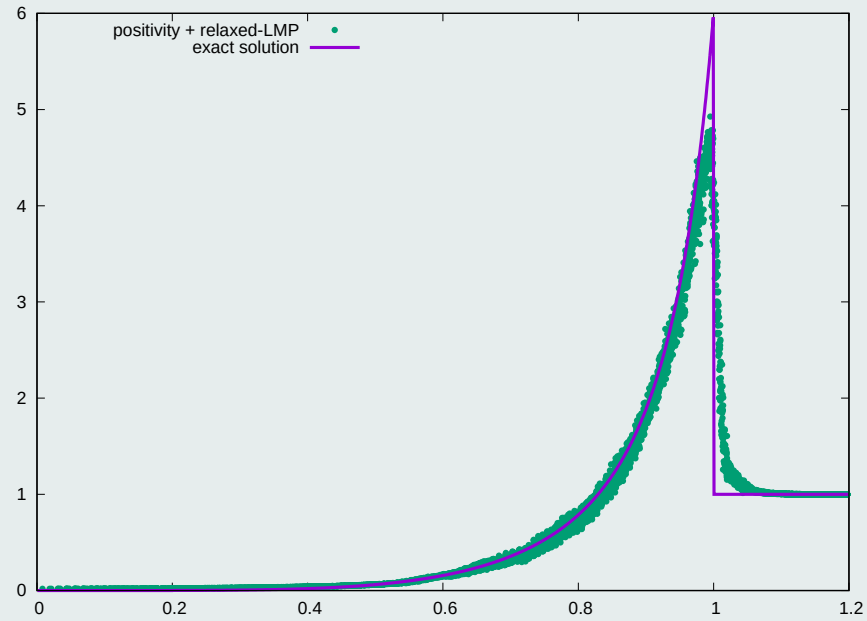


(b) Density profile

Figure: $\mathbb{P}^5$-DG/FV with positivity and relaxed-LMP on a 271 cells mesh

# Mach 20 hypersonic flow over half cylinder

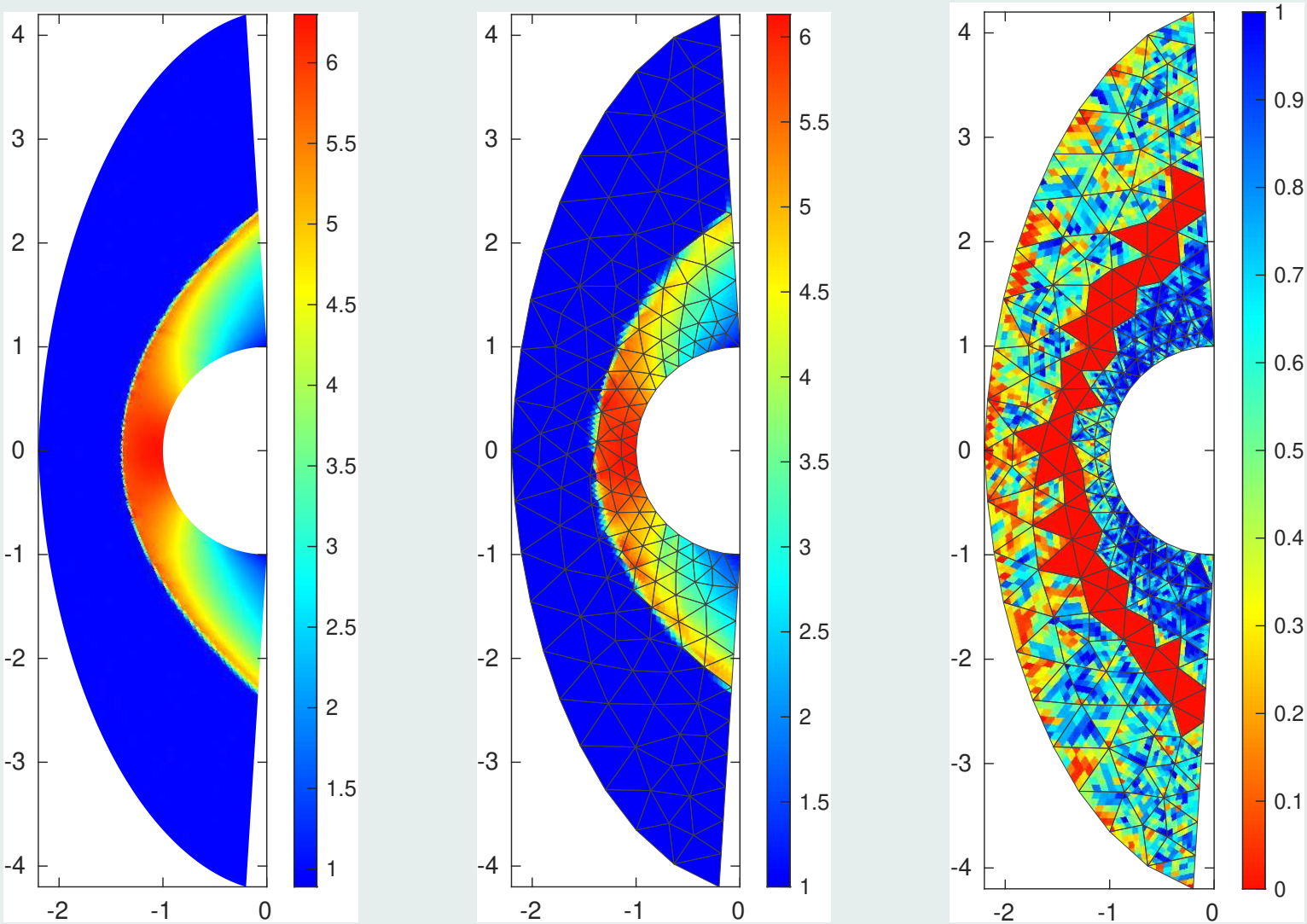

(a) $\mathbb{P}^0$ on 25266 cells (b) $\mathbb{P}^5$ on 292 cells (c) $\mathbb{P}^5$ on 292 cells

Figure: Monolithic subcell DG/FV scheme: density and blending coefficients

## 2D non-linear shallow water equations - prebalanced formulation

- $\partial_t \boldsymbol{V} + \nabla_x \cdot \boldsymbol{F}(\boldsymbol{V}, b) = \boldsymbol{B}(\boldsymbol{V}, \nabla_x b)$
- $\boldsymbol{V} = \begin{pmatrix} \eta \\ \boldsymbol{q} \end{pmatrix}$ conservative variables
- $\boldsymbol{B}(\boldsymbol{V}, \partial_x b) = \begin{pmatrix} 0 \\ -g\,\eta\,\nabla_x b \end{pmatrix}$ source term
- $\boldsymbol{F}(\boldsymbol{V}, b) = \begin{pmatrix} \boldsymbol{q} \\ \dfrac{\boldsymbol{q} \otimes \boldsymbol{q}}{\eta - b} + \dfrac{1}{2} g \left(\eta^2 - 2\,\eta\,b\right) I_d \end{pmatrix}$ flux function

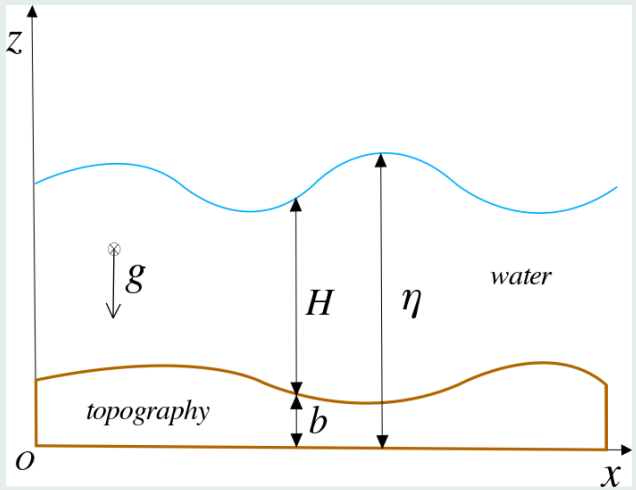


## Monolithic subcell DG/FV scheme property

- Positivity-preservation of the water height $H = \eta - b$, at the subcell scale
- Well-balancing property, at the subcell scale

## Well-balancing property — *Sacha Cardonna*

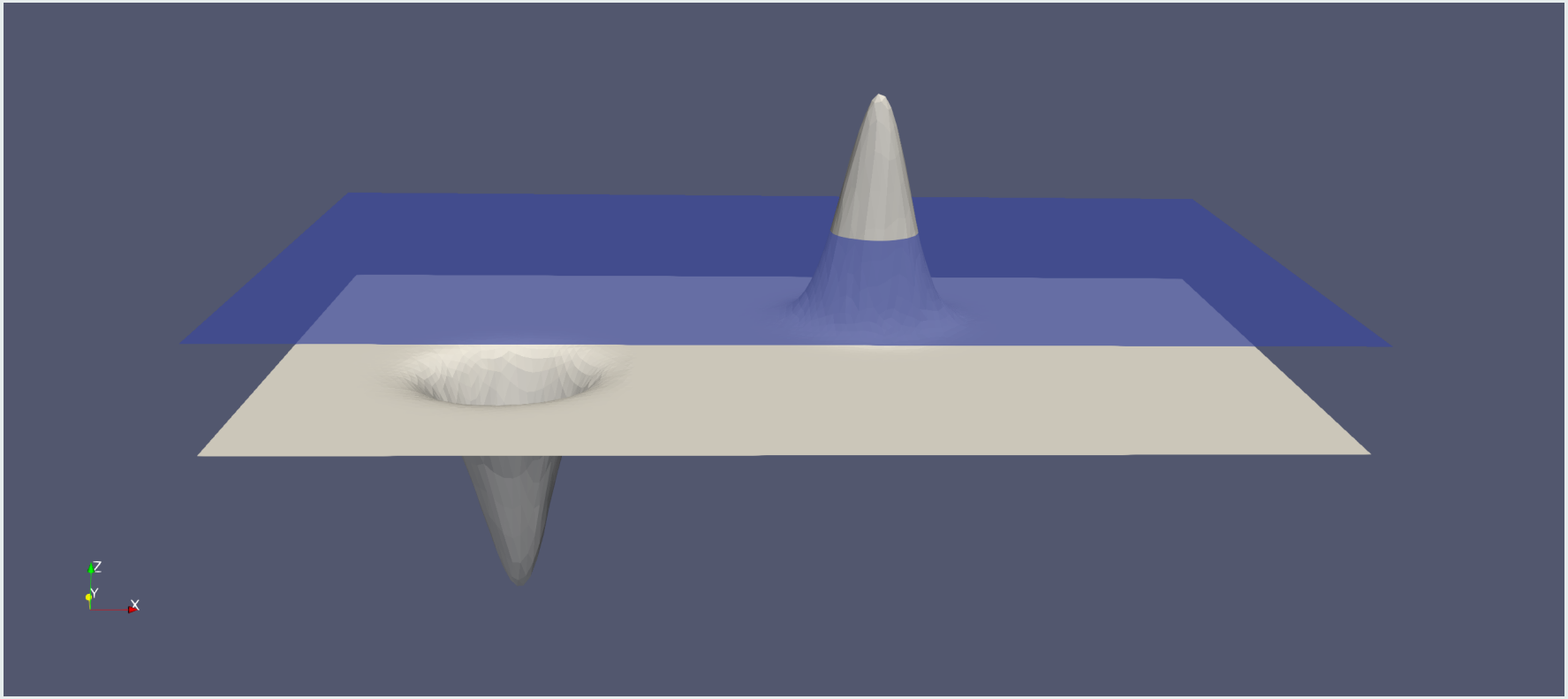


Figure : $\mathbb{P}^2$-DG/FV with positivity and relaxed-LMP on a 2064 cells mesh

# Dam break problem

**Sacha Cardonna**

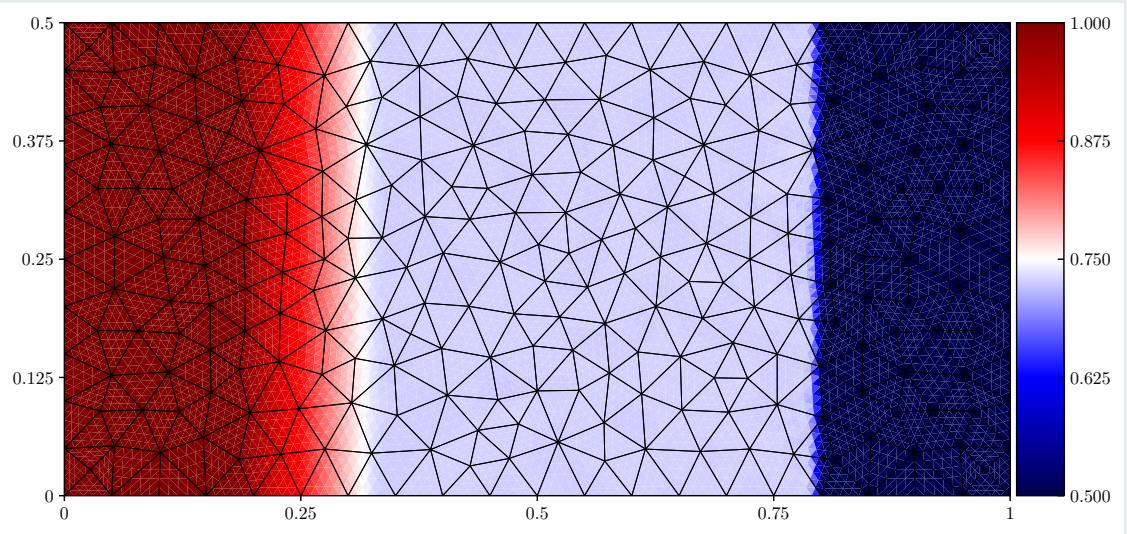


(a) Elevation map

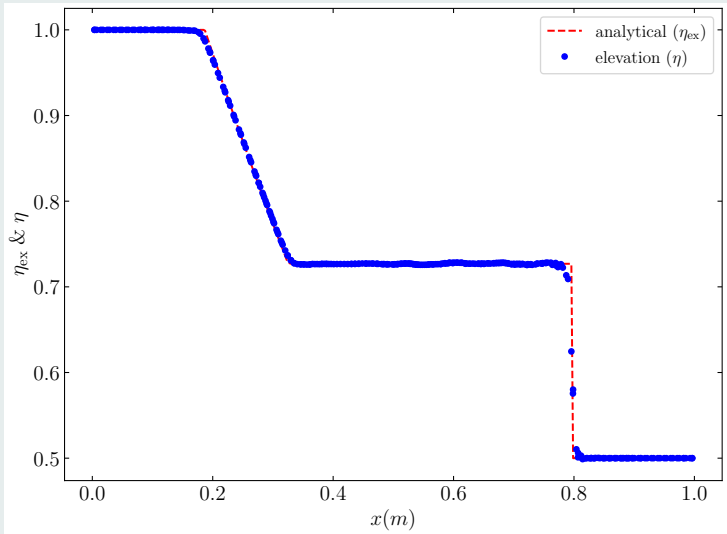


(b) Elevation profile

Figure : $\mathbb{P}^5$-DG/FV with positivity and relaxed-LMP on a 506 cells mesh

# Rock-wave interaction

**Sacha Cardonna**

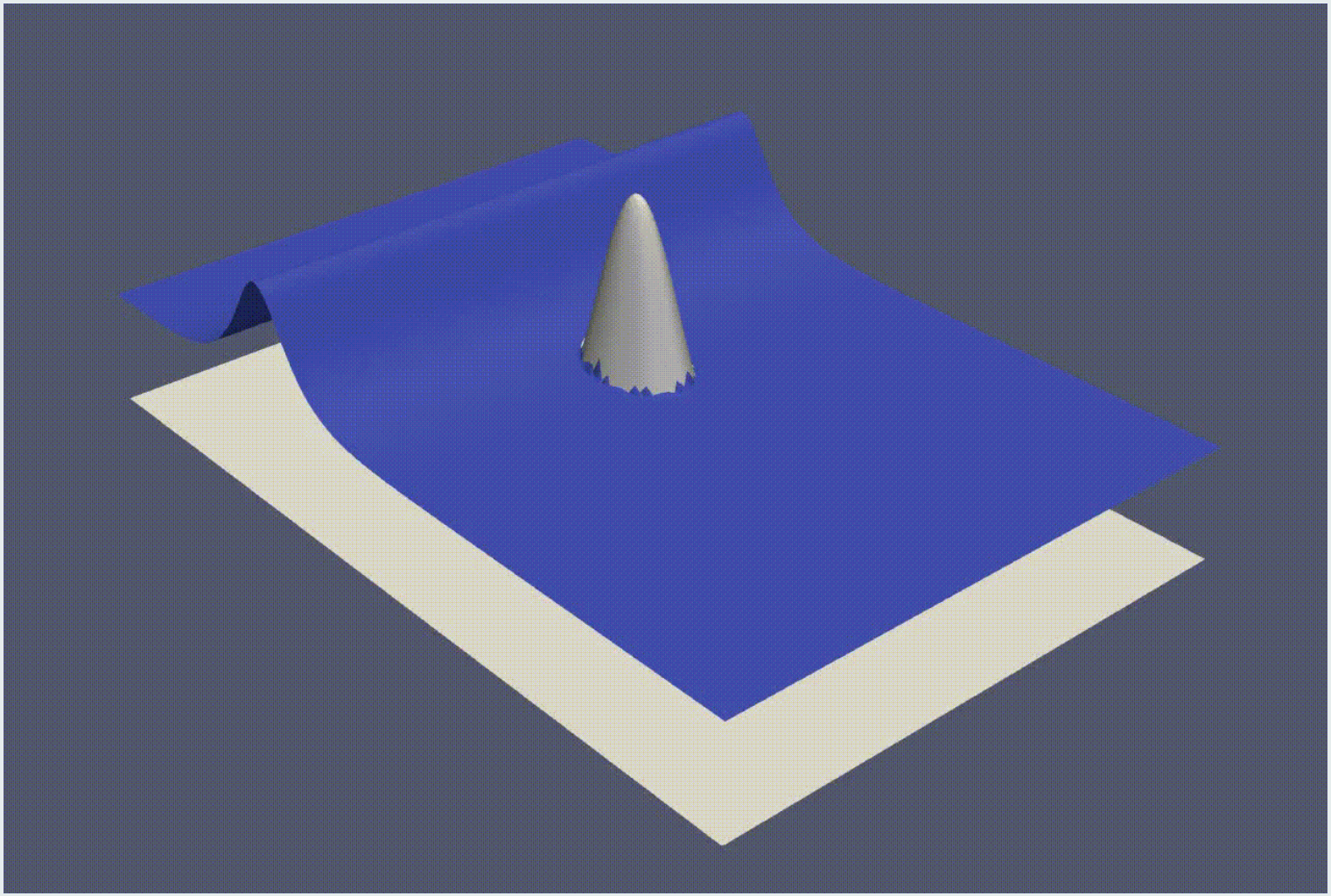

Figure : $\mathbb{P}^6$-DG/FV with positivity and relaxed-LMP on a 1018 cells mesh

# Rock-wave interaction

**Sacha Cardonna**

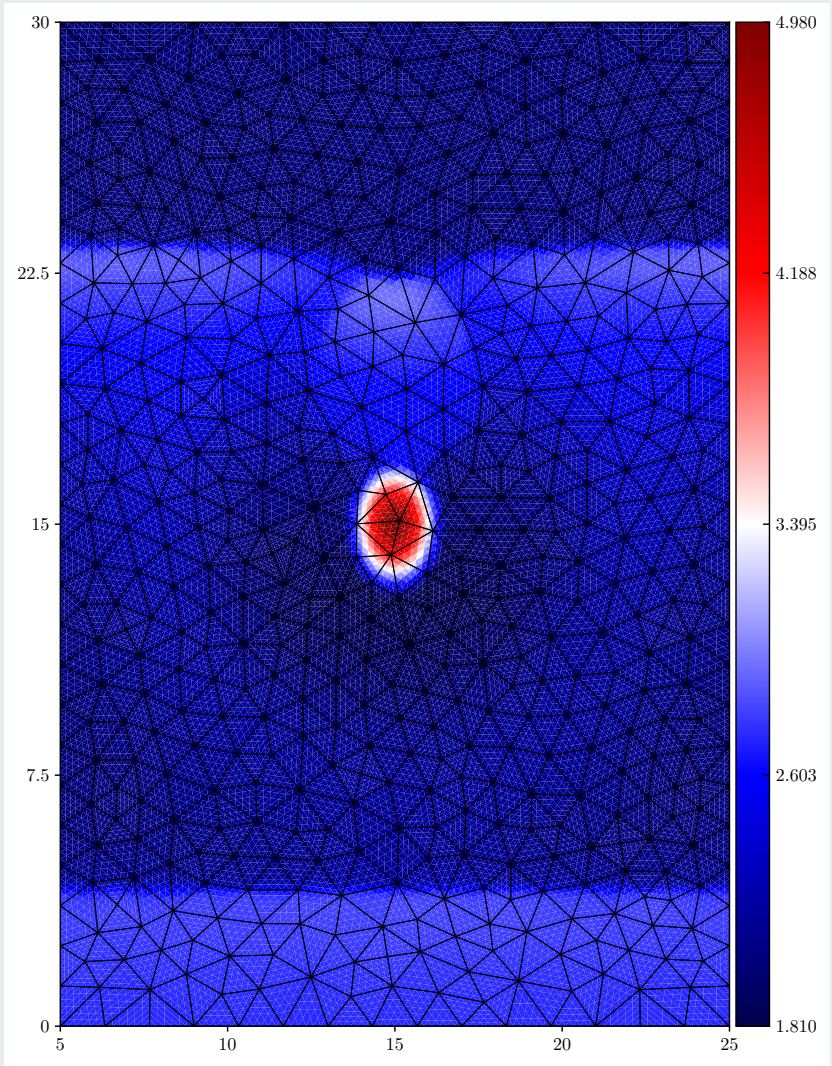


(a) Surface elevation

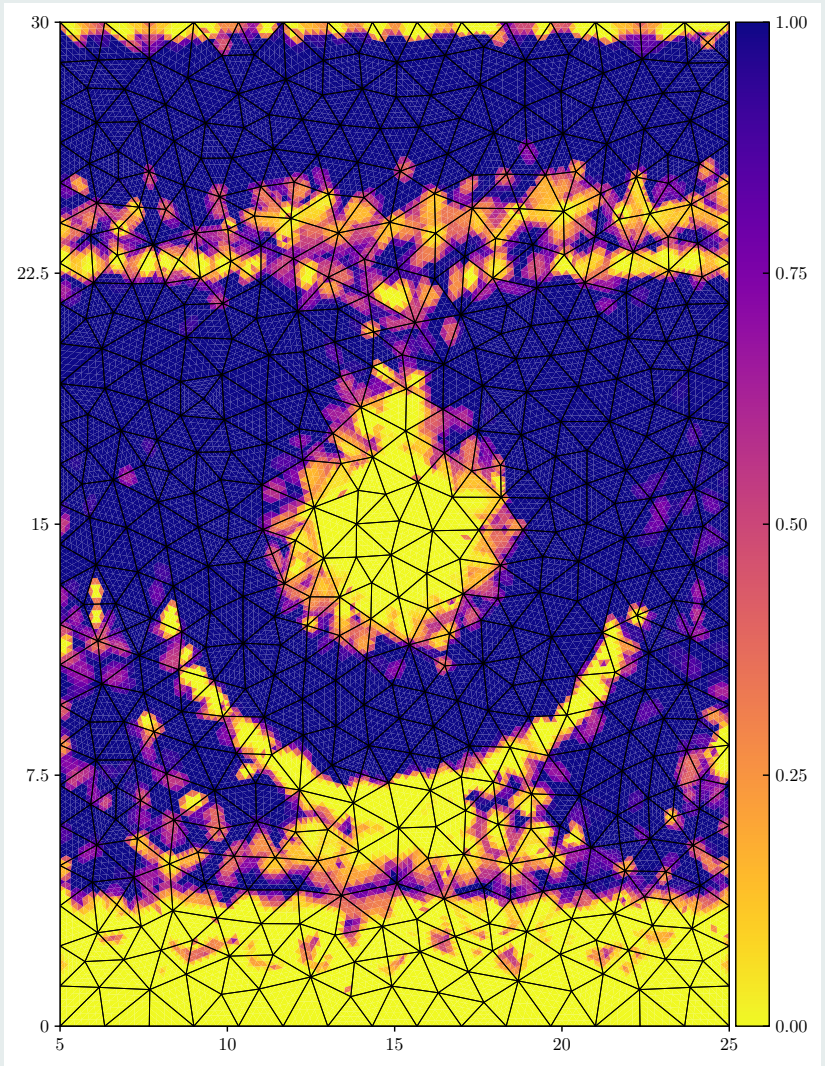


(b) Blending coefficients

Figure : $\mathbb{P}^6$-DG/FV with positivity and relaxed-LMP on a 1018 cells mesh

## Monolithic local subcell DG/FV scheme

- Reformulate DG schemes as subgrid FV-like schemes:
  - regardless the type of mesh used
  - regardless the space dimension (***in theory***...)
  - regardless the cell subdivision ($N_s \geq N_k$)
- Combine high-order reconstructed fluxes and 1$^{st}$-order FV fluxes
  - ensuring a maximum or positivity preserving principle at the subcell scale
  - ensuring different entropy stability inequalities
  - reducing significantly the apparition of spurious oscillations
  - preserving the very accurate subcell resolution of DG schemes

## Some of our undergoing works on that matter

- Application to shallow-water flows coupled with a floating object

  ↪ **Sacha Cardonna** and **F. Marche**

- Extension to multi-dimensional nodal solvers and Lagrangian frame

  ↪ **W. Boscheri**, **R. Loubère** and **P.-H. Maire**

# Articles on this topic


- **F.V**, *A Posteriori Correction of High-Order DG Scheme through Subcell Finite Volume Formulation and Flux Reconstruction.* JCP, 2018.
- **A. HAIDAR**, **F. MARCHE** AND **F.V**, *A posteriori Finite-Volume local subcell correction of high-order discontinuous Galerkin schemes for the nonlinear shallow-water equations*. JCP, 2022.
- **F.V** AND **R. ABGRALL**, *A posteriori local subcell correction of DG schemes through Finite Volume reformulation on unstructured grids.* SIAM SISC, 2023.
- **A. HAIDAR**, **F. MARCHE** AND **F.V**, *Free-boundary problems for wave-structure interactions in shallow-water: DG-ALE description and local subcell correction*. JSC, 2023.
- **A. HAIDAR**, **F. MARCHE** AND **F.V**, *A robust DG-ALE formulation for nonlinear shallow-water interactions with a floating object*. JSC, 2024.
- **F.V**, *Monolithic local subcell DG/FV convex property preserving scheme on unstructured grids and entropy consideration.* JCP, 2024.

# 1st PICASSO conference - March 24-26 Málaga, Spain

Restricted number of seats, but some are still available!

https://indico.math.cnrs.fr/e/PICASSO

*Pleanary lecturers:*

S. Clain (Univ. Coimbra, PT)
S. Gavriliuk (Univ. Marseille, FR)
P. Mulet (univ. Valencia, SP)
M. Ricchiuto (Univ. Bordeaux, FR)
E. Fernández-Nieto (Univ. Sevilla, SP)


# International Research Project - PICASSO – 2025 - 2029

PICASSO: "hyPerbolIC models, numerical AnalysiS & Scientific computation"

$\Longrightarrow$ enhance the relationship between France - Portugal - Spain

**Goal:** multiply the opportunities of collaboration (workshop, visits, co-mentoring, . . . )

**Animation:** C. Berthon, C. Chalons, R. Loubère, S. Clain, A. Duarte, C. Pares, T. Morales de Luna, M. Castro

Soon a web-site will be available.

# 1st PICASSO conference - March 24-26 Málaga, Spain

Restricted number of seats, but some are still available!

https://indico.math.cnrs.fr/e/PICASSO

*Pleanary lecturers:*

S. Clain (Univ. Coimbra, PT)
S. Gavriliuk (Univ. Marseille, FR)
P. Mulet (univ. Valencia, SP)
M. Ricchiuto (Univ. Bordeaux, FR)
E. Fernández-Nieto (Univ. Sevilla, SP)


# International Research Project - PICASSO – 2025 - 2029

PICASSO: "hyPerbolIC models, numerical AnalysiS & Scientific computation"

$\Longrightarrow$ enhance the relationship between France - Portugal - Spain

**Goal:** multiply the opportunities of collaboration (workshop, visits, co-mentoring, . . . )

**Animation:** C. Berthon, C. Chalons, R. Loubère, S. Clain, A. Duarte, C. Pares, T. Morales de Luna, M. Castro

Soon a web-site will be available.

## Different cell subdivisions $\mathbb{P}^3$

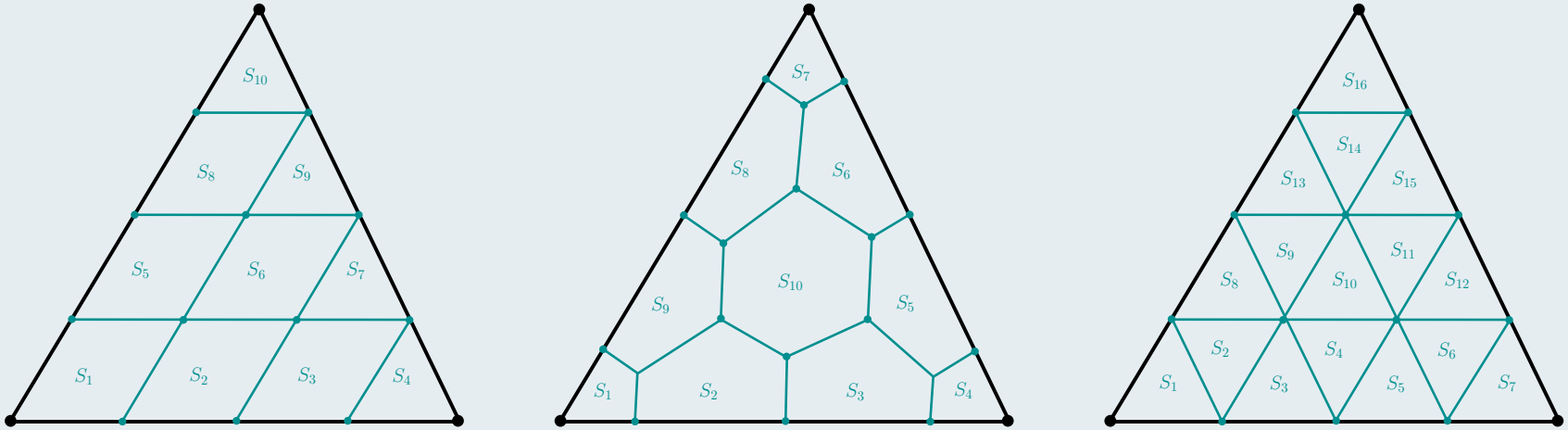


Figure : Examples of easily generalizable subdivisions for a triangle cell

## DG is DG

- **Only the functional space matters**
- **The cell subdivision has no influence on the resulting scheme**
- **Even in the case where** $N_s > N_k$

# Rotation of a composite signal after one full rotation

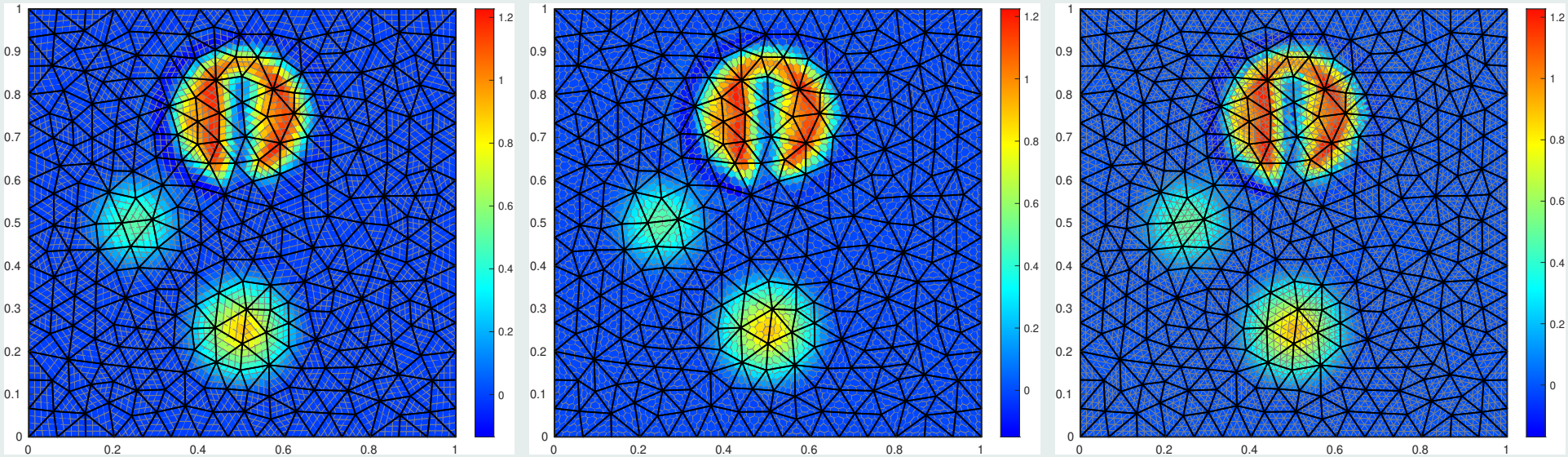

(a) Cartesian subdivision (b) Polygonal subdivision (c) Triangular subdivision

Figure : $\mathbb{P}^3$ reconstructed flux FV schemes on 576 cells: subcells mean values

# Rotation of a composite signal after one full rotation

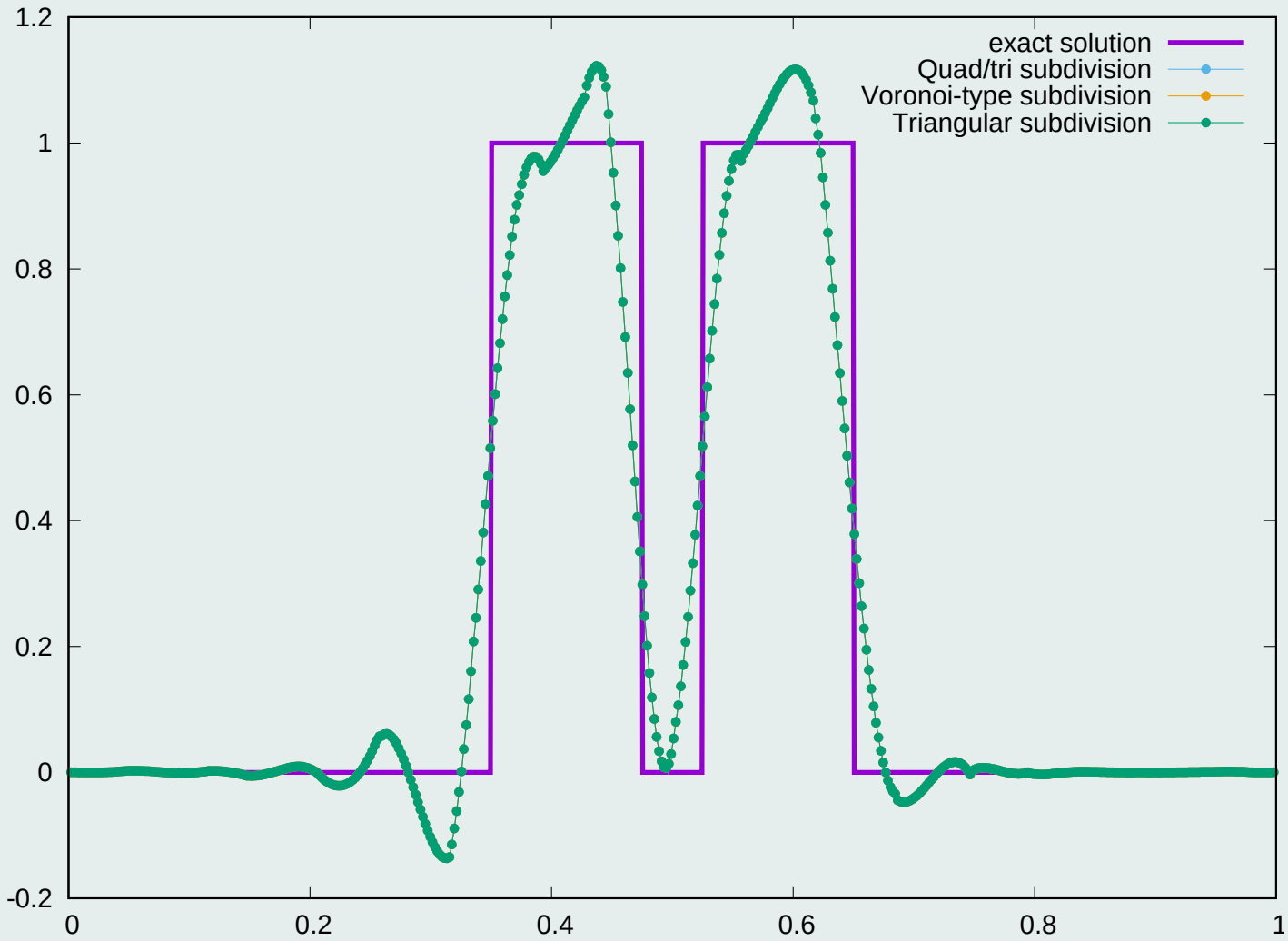


Figure : Reconstructed flux FV schemes on 576 cells: solution profiles for $y = 0.75$

## Submean values

- $\overline{u}_m^c = \dfrac{1}{|S_m^c|} \displaystyle\sum_{q=1}^{N_k} u_q^c \int_{S_m^c} \sigma_q \, \mathrm{d}V \quad \Longrightarrow \quad \boxed{\overline{\mathrm{U}}_c = P_c \, \mathrm{U}_c}$
- $(\overline{\mathrm{U}}_c)_m = \overline{u}_m^c$ Submean values
- $(P_c)_{mp} = \dfrac{1}{|S_m^c|} \displaystyle\int_{S_m^c} \sigma_p \, \mathrm{d}V$ Projection matrix

$$\Longrightarrow \quad \boxed{\frac{\mathrm{d}\,\overline{\mathrm{U}}_c}{\mathrm{d}t} = P_c \, M_c^{-1} \, \Phi_c}$$

## Admissibility of the cell sub-partition into subcells

- $P_c^{\mathrm{t}} P_c$ **has to be non-singular**

$$\Longrightarrow \quad \boxed{\mathrm{U}_c = (P_c^{\mathrm{t}} P_c)^{-1} P_c^{\mathrm{t}} \, \overline{\mathrm{U}}_c}$$ Least square procedure

- If $N_s = N_k$, $\overline{\mathrm{U}}_c = P_c \, \mathrm{U}_c \iff \mathrm{U}_c = P_c^{-1} \overline{\mathrm{U}}_c$

# Blended Riemann intermediate states

- $$\widetilde{u_{mp}}^{-} = \overline{u}_m^{c,n} - \frac{\mathcal{F}_{mp}^{\mathrm{FV}} - \boldsymbol{F}(\overline{u}_m^{c,n}) \cdot \boldsymbol{n}_{mp}}{\gamma_{mp}} - \theta_{mp}\frac{\Delta F_{mp}}{\gamma_{mp}}$$
$$= \underbrace{\frac{\overline{u}_m^{c,n} + \overline{u}_p^{v,n}}{2} - \frac{\left(\boldsymbol{F}(\overline{u}_p^{v,n}) - \boldsymbol{F}(\overline{u}_m^{c,n})\right) \cdot \boldsymbol{n}_{mp}}{2\,\gamma_{mp}}}_{u_{mp}^{*,\mathrm{FV}}} - \theta_{mp}\frac{\Delta F_{mp}}{\gamma_{mp}}$$

- $$\widetilde{u_{mp}}^{\pm} = u_{mp}^{*,\mathrm{FV}} \pm \theta_{mp}\frac{\Delta F_{mp}}{\gamma_{mp}} \quad \Longrightarrow \quad u_{mp}^{*,\mathrm{FV}} = \frac{1}{2}\left(\widetilde{u_{mp}}^{-} + \widetilde{u_{mp}}^{+}\right)$$

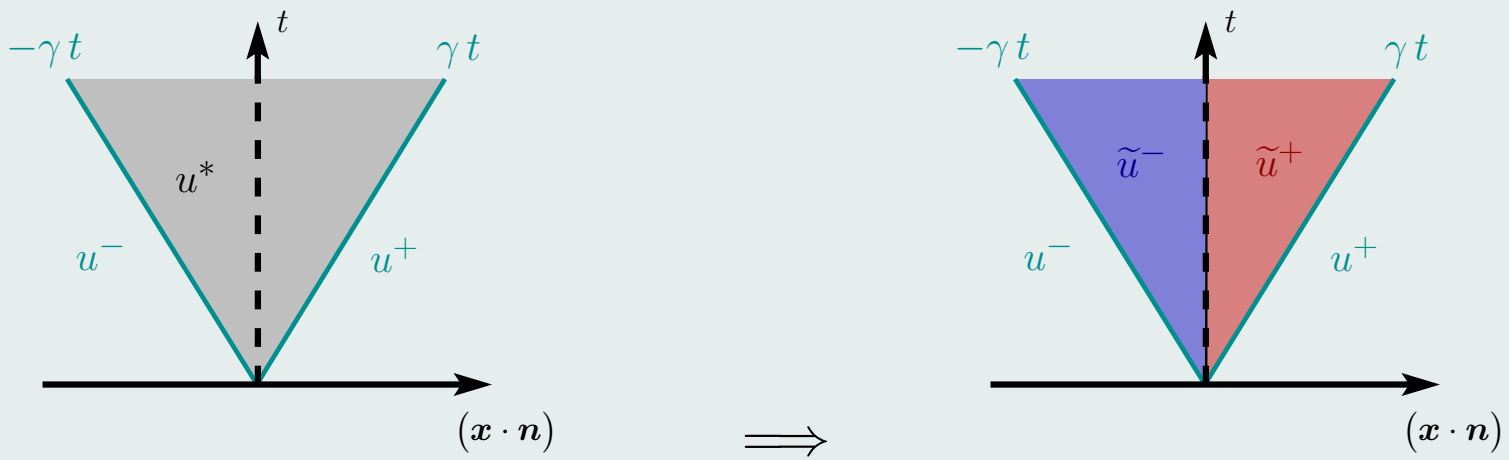


(a) 1st-order situation (b) Blended flux situation

# Double rarefaction test case 10 cells

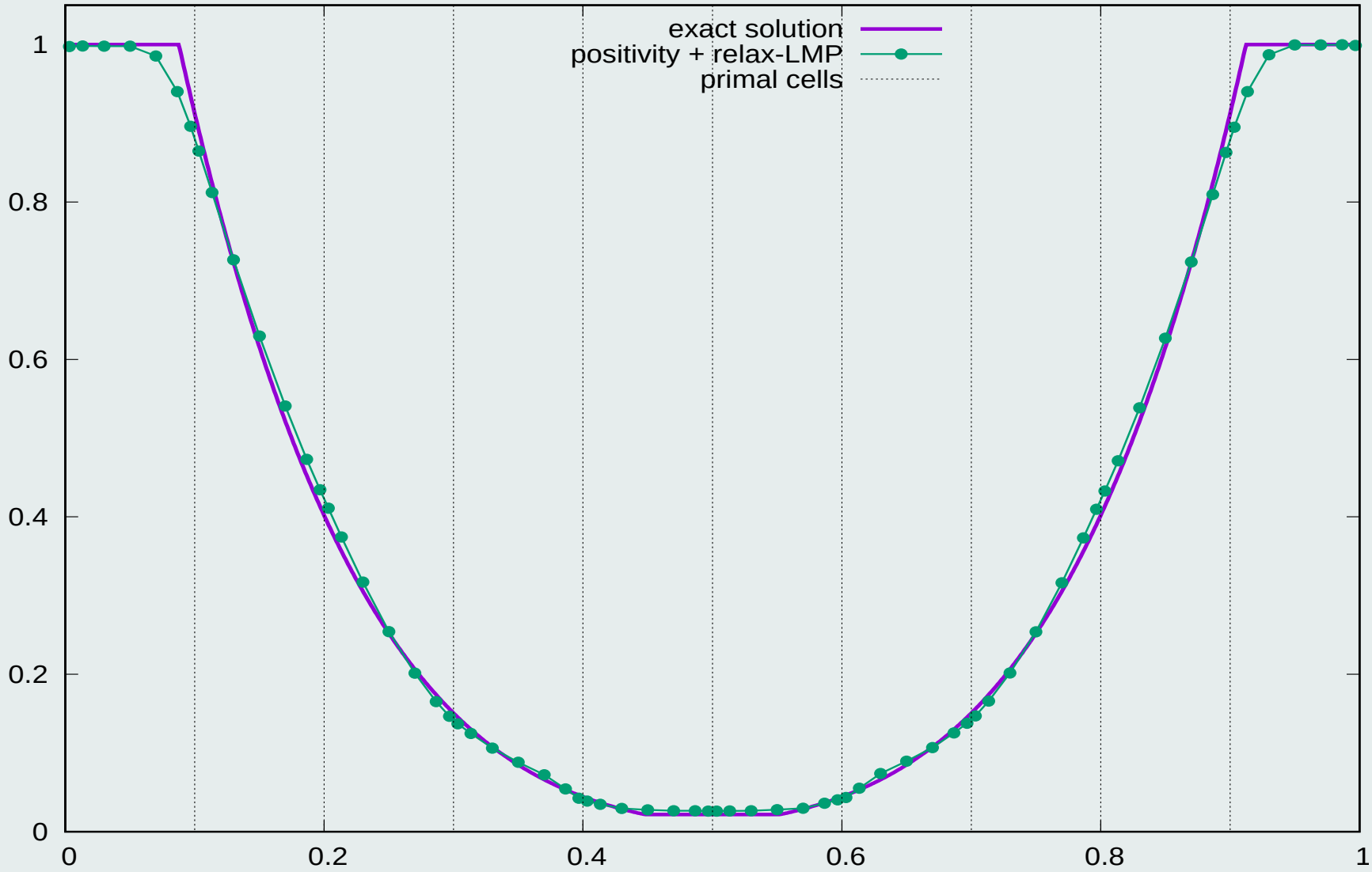


Figure: $\mathbb{P}^6$-DG/FV scheme with GMP and relaxed-LMP: submean values

# Shock acoustic-wave interaction test case 200 cells

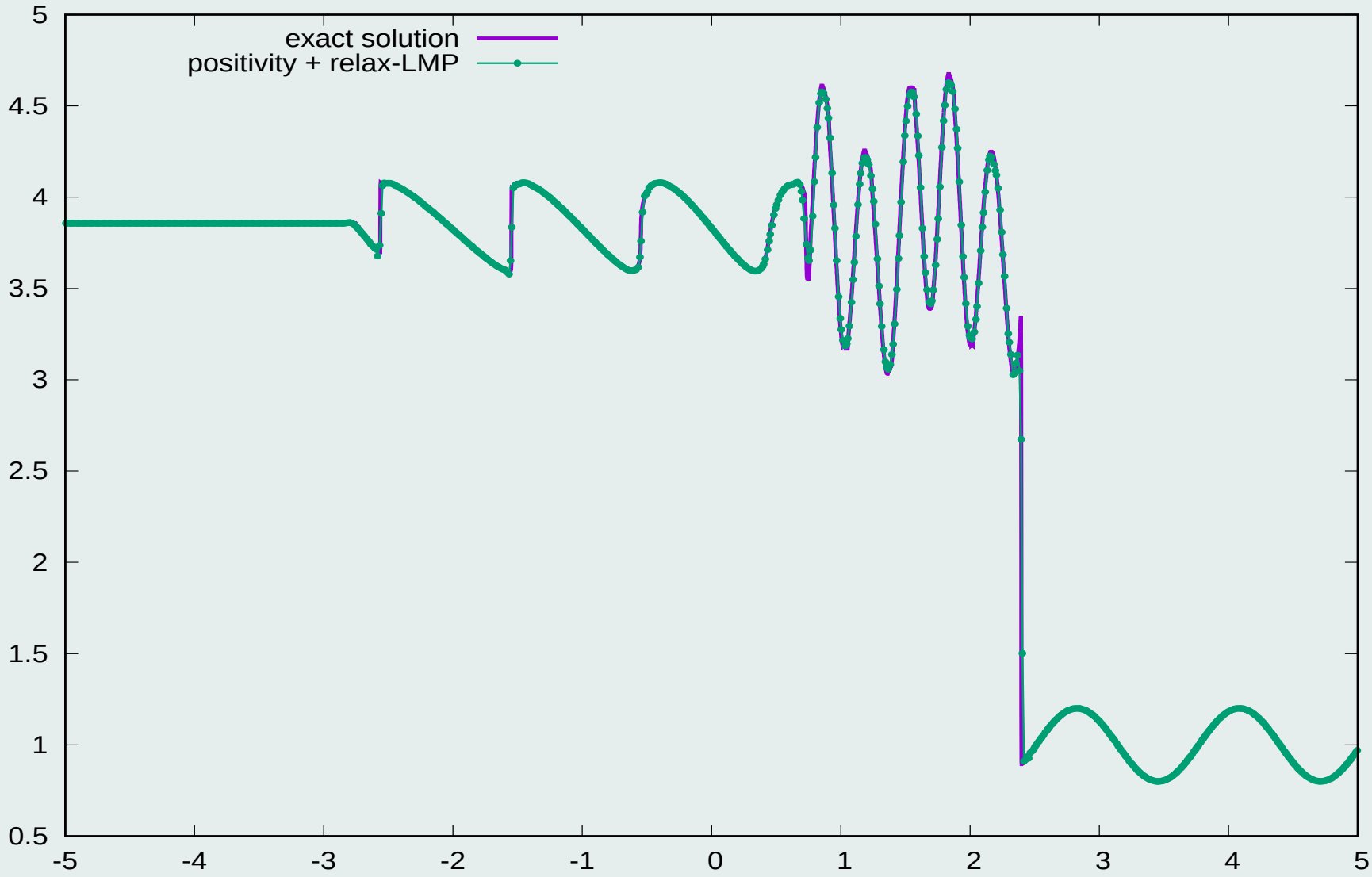


Figure: $\mathbb{P}^3$-DG/FV scheme with GMP and relaxed-LMP: HLL-C numerical flux

# Mach 3 forward-facing step

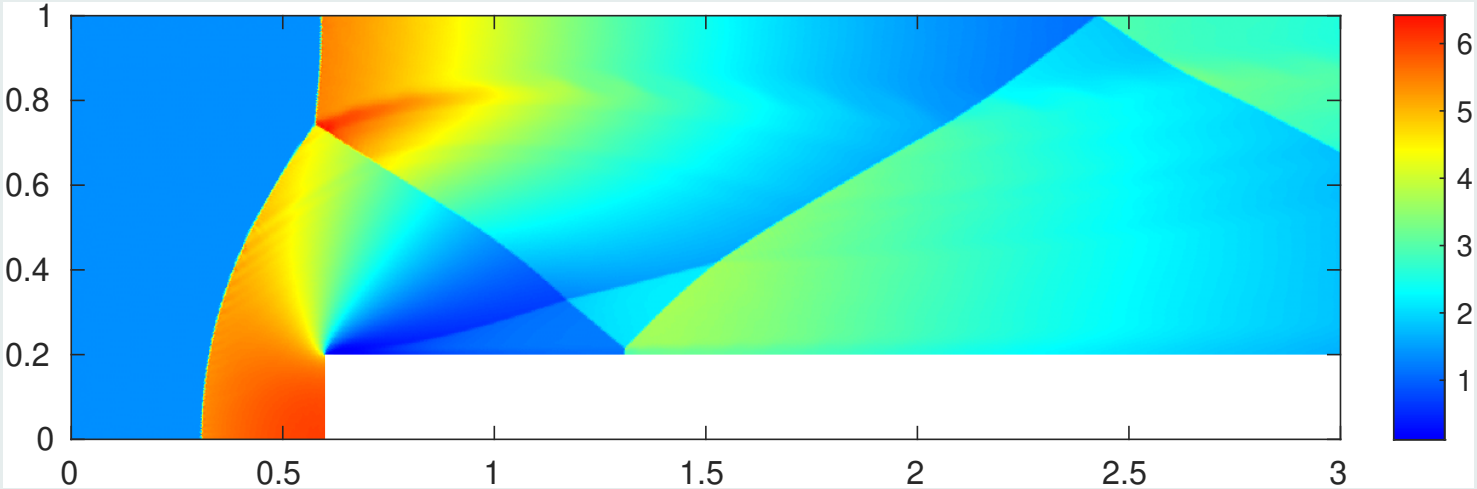


(a) $\mathbb{P}^1$ on 84108 cells

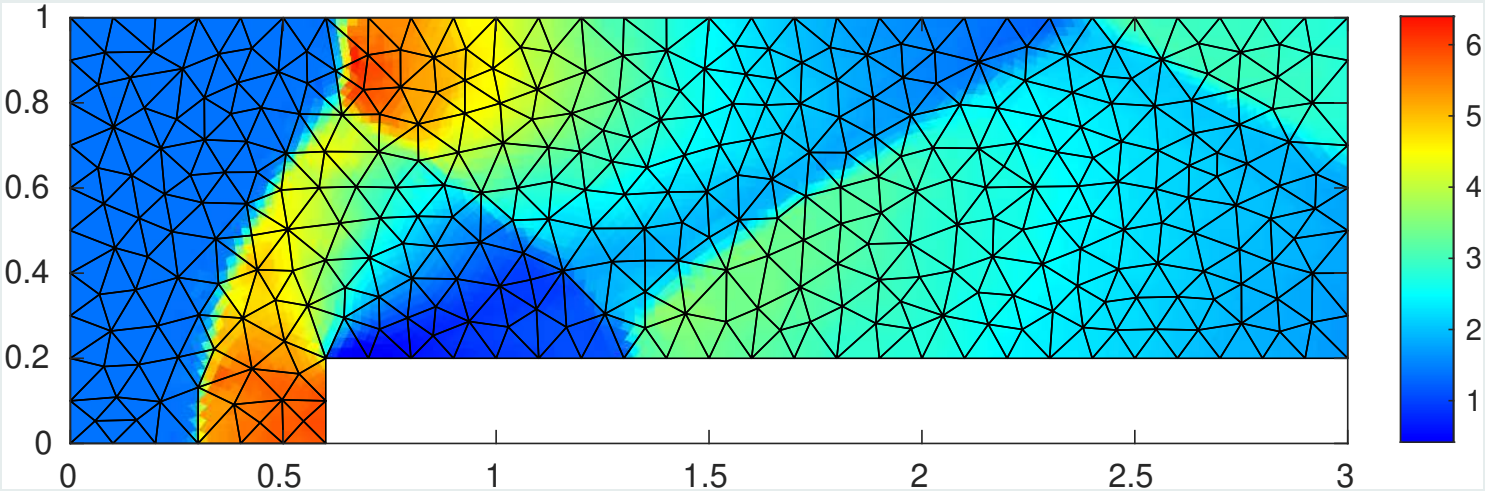


(b) $\mathbb{P}^3$ on 680 cells

Figure: Monolithic subcell DG/FV scheme: subcell density mean values